Z_2 topological order near the Neel state on the square lattice

Institut für Theoretische Physik
Universität Heidelberg
April 28, 2017

Subir Sachdev

Talk online: sachdev.physics.harvard.edu

PERIMETER INSTITUTE FOR THEORETICAL PHYSICS

NSF

PHYSICS
VE RI TAS
HARVARD

Shubhayu Chatterjee

Mathias Scheurer

Alex Thomson

1. Z_2 lattice gauge theory and topological order

2. CP^1 theory of square lattice antiferromagnets and Z_2 topological order

3. Z_2 topological order and the volume enclosed by the Fermi surface

Z_2 lattice gauge theory (Wegner, 1971)

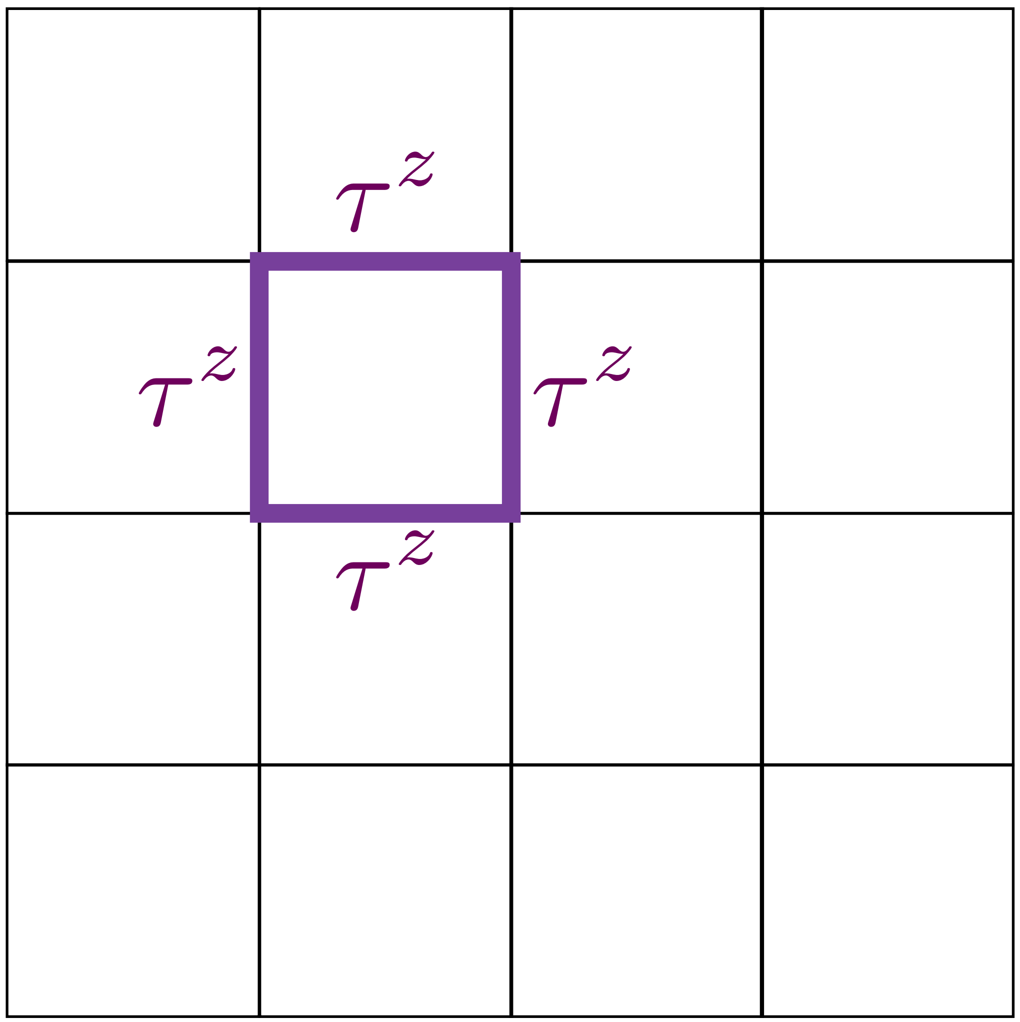

$$H = -\sum_{\square} \tau^z \tau^z \tau^z \tau^z - g \sum_i \tau^x$$

$G_i =$

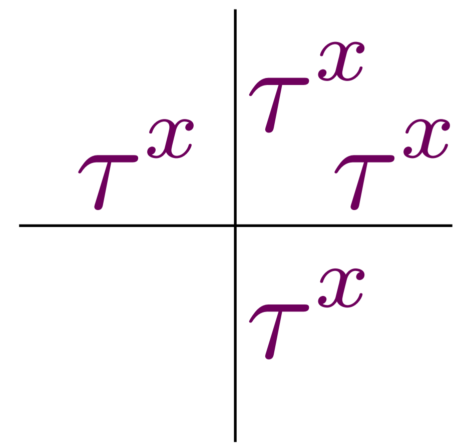

Gauss's Law: $\quad [H, G_i] = 0 \quad , \quad G_i = 1$

Z_2 lattice gauge theory

(Wegner, 1971)

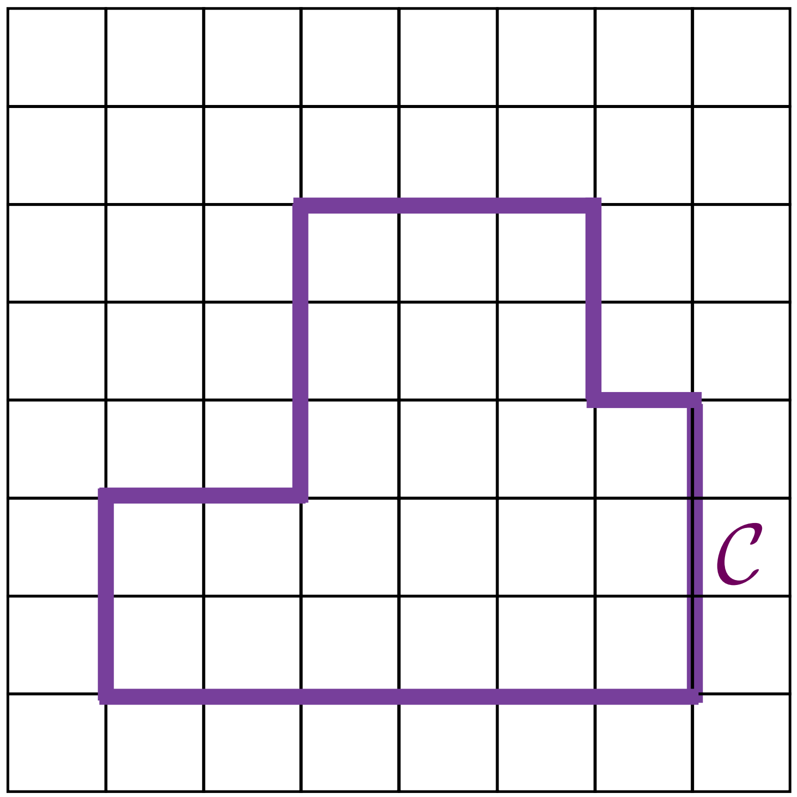

$$W_{\mathcal{C}} = \prod_{\mathcal{C}} \tau^z$$

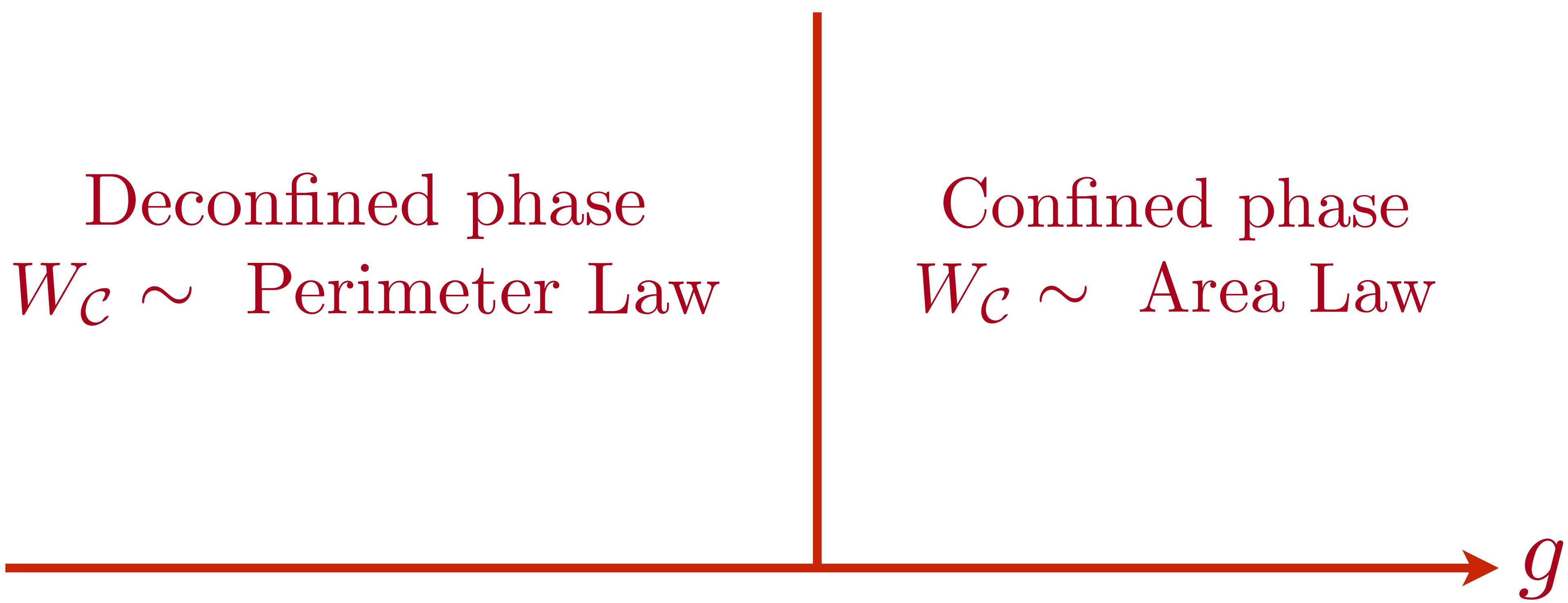

Topological order

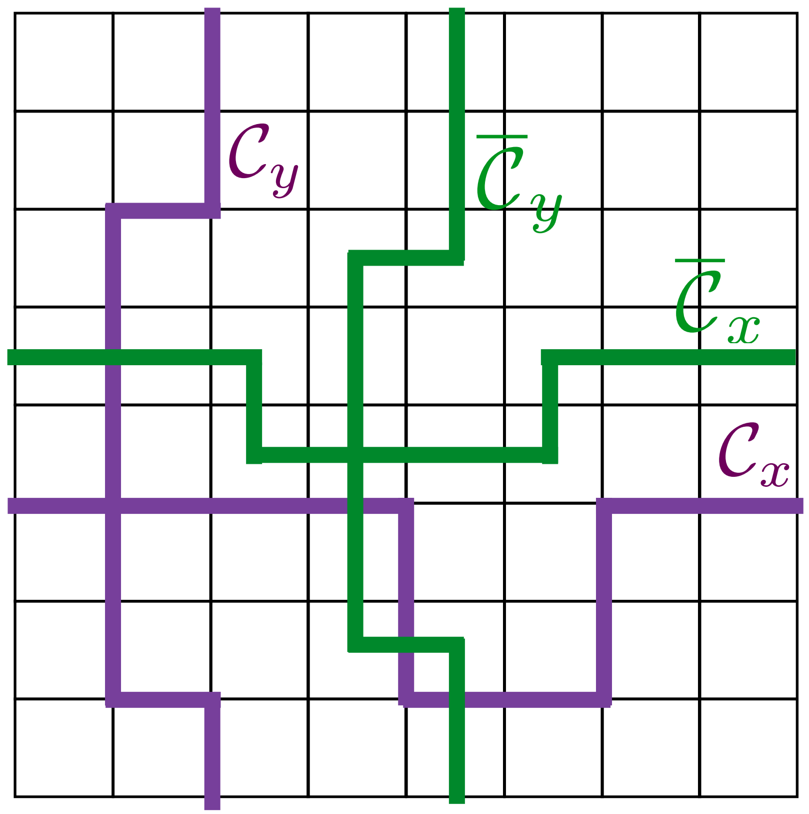

$$V_x = \prod_{\overline{\mathcal{C}}_x} \tau^x \quad , \quad V_y = \prod_{\overline{\mathcal{C}}_y} \tau^x$$

$$W_x = \prod_{\mathcal{C}_x} \tau^z \quad , \quad W_y = \prod_{\mathcal{C}_y} \tau^z$$

$$V_x W_y = -W_y V_x \quad , \quad V_y W_x = -W_x V_y$$

and all other pairs commute.

On a torus, there are two additional independent operators, V_x and V_y which commute with the Hamiltonian:

$$[H, V_x] = [H, V_y] = 0$$

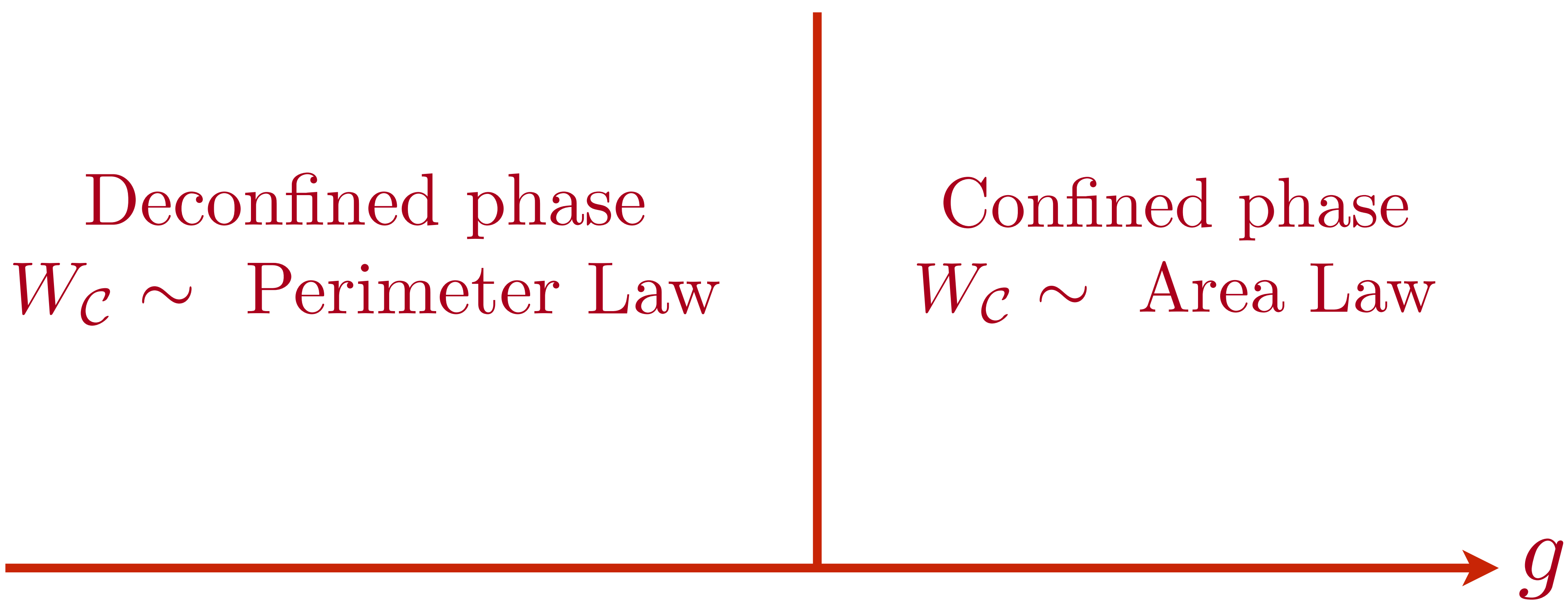

Topological order

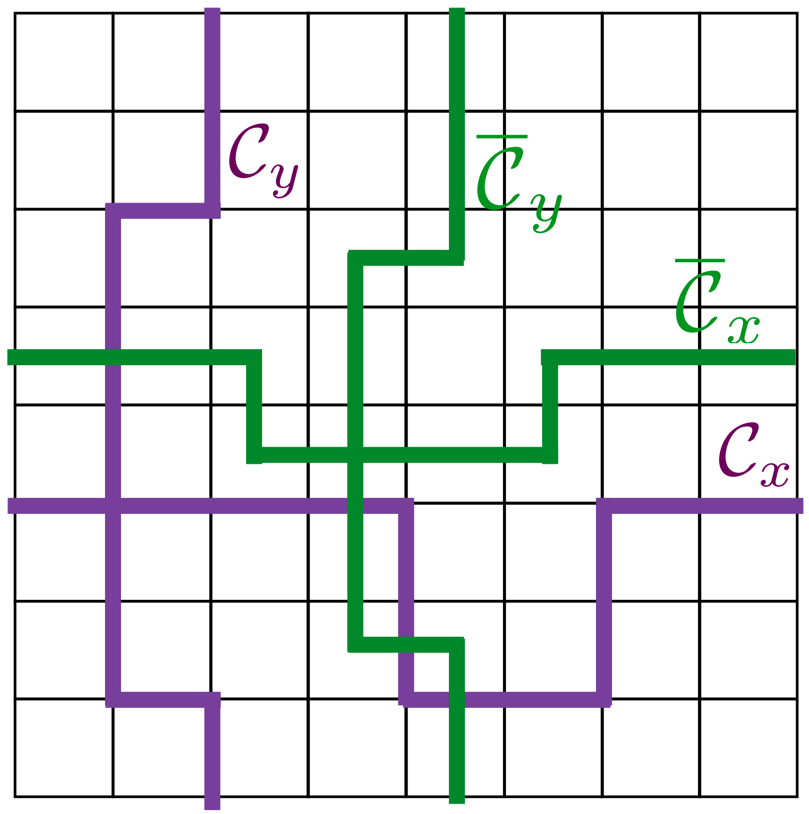

$$V_x = \prod_{\overline{\mathcal{C}}_x} \tau^x \quad , \quad V_y = \prod_{\overline{\mathcal{C}}_y} \tau^x$$

$$W_x = \prod_{\mathcal{C}_x} \tau^z \quad , \quad W_y = \prod_{\mathcal{C}_y} \tau^z$$

$$V_x W_y = -W_y V_x \quad , \quad V_y W_x = -W_x V_y$$

and all other pairs commute.

On a torus, there are two additional independent operators, V_x and V_y which commute with the Hamiltonian:

$$[H, V_x] = [H, V_y] = 0$$

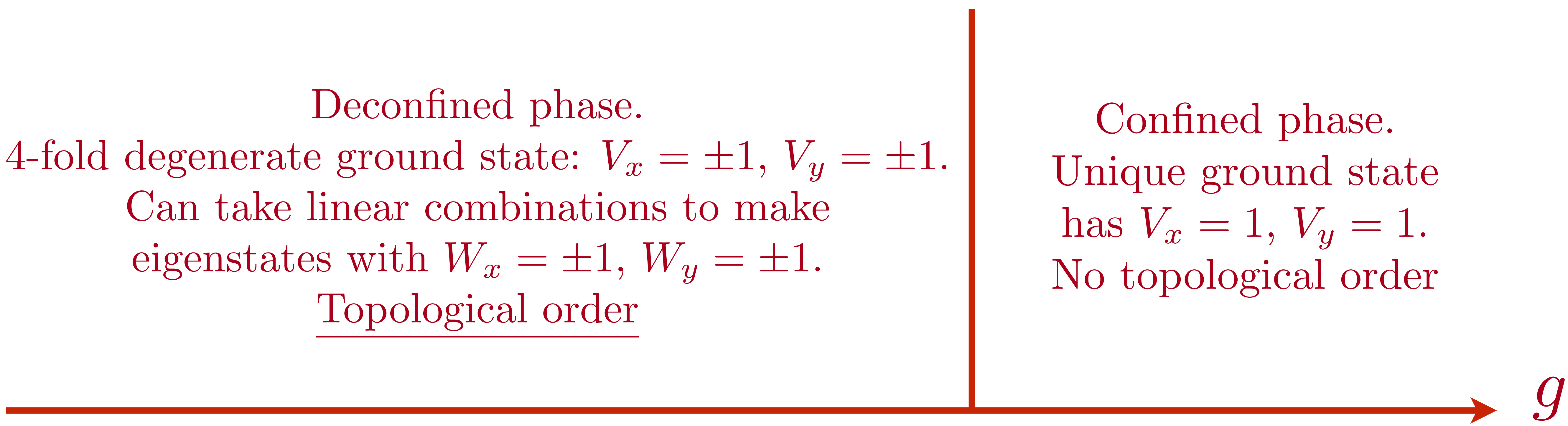

Topological order

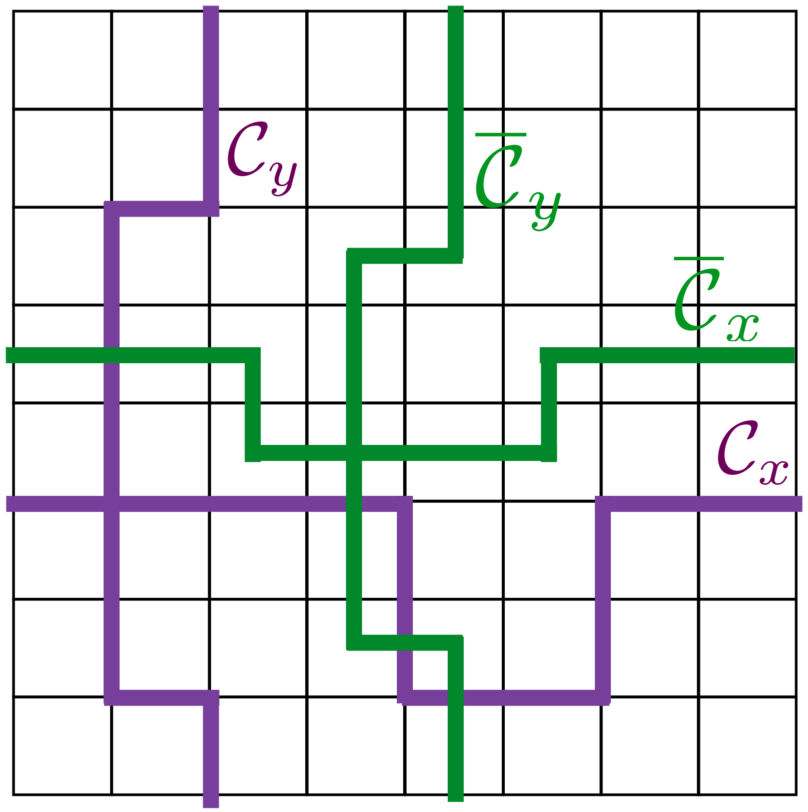

$$V_x = \prod_{\overline{\mathcal{C}}_x} \tau^x \quad , \quad V_y = \prod_{\overline{\mathcal{C}}_y} \tau^x$$

$$W_x = \prod_{\mathcal{C}_x} \tau^z \quad , \quad W_y = \prod_{\mathcal{C}_y} \tau^z$$

$$V_x W_y = -W_y V_x \quad , \quad V_y W_x = -W_x V_y$$

and all other pairs commute.

On a torus, there are two additional independent operators, V_x and V_y which commute with the Hamiltonian:

$$[H, V_x] = [H, V_y] = 0$$

Topological phase has degenerate states with Z_2 flux $W = \pm 1$ through the holes of the torus

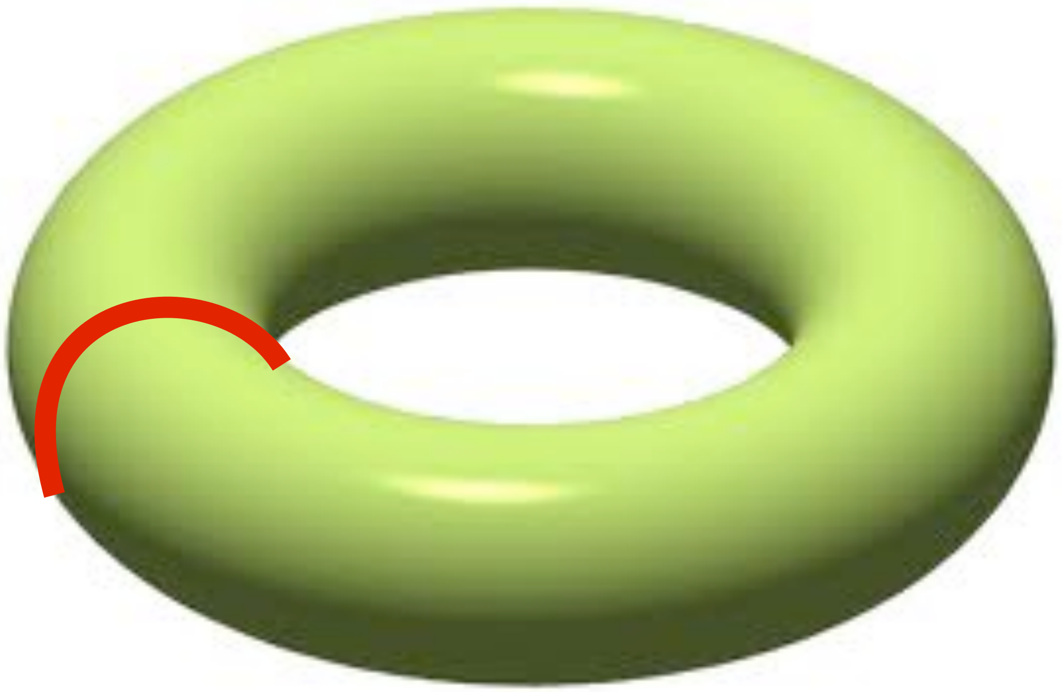

(N. Read and S.S., 1991)

Topological order

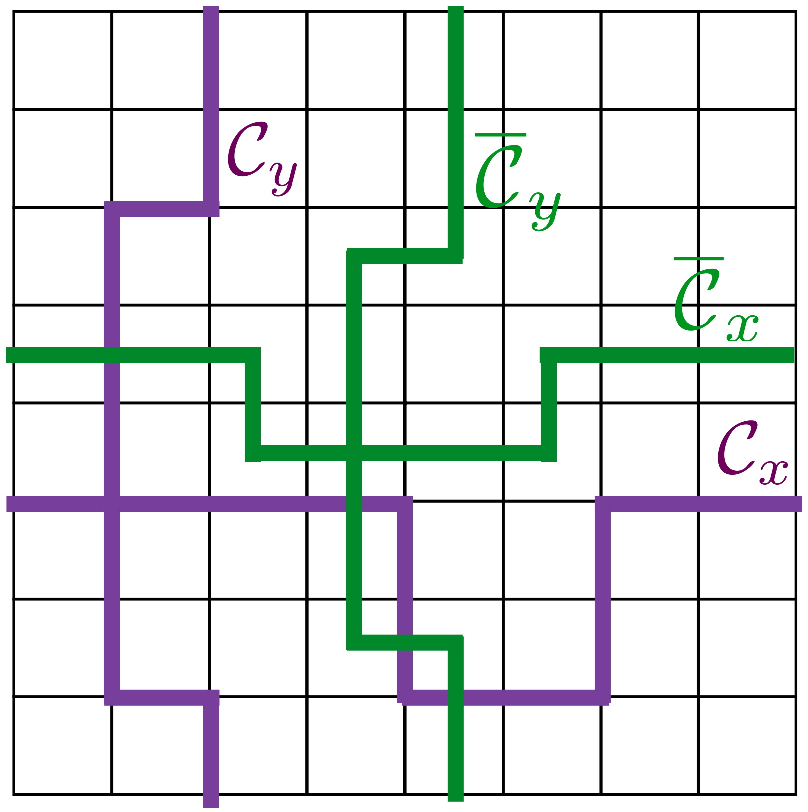

$$V_x = \prod_{\overline{\mathcal{C}}_x} \tau^x \quad , \quad V_y = \prod_{\overline{\mathcal{C}}_y} \tau^x$$

$$W_x = \prod_{\mathcal{C}_x} \tau^z \quad , \quad W_y = \prod_{\mathcal{C}_y} \tau^z$$

$$V_x W_y = -W_y V_x \quad , \quad V_y W_x = -W_x V_y$$

and all other pairs commute.

On a torus, there are two additional independent operators, V_x and V_y which commute with the Hamiltonian:

$$[H, V_x] = [H, V_y] = 0$$

Deconfined phase.
4-fold degenerate ground state: $V_x = \pm 1$, $V_y = \pm 1$.
Can take linear combinations to make eigenstates with $W_x = \pm 1$, $W_y = \pm 1$.
Topological order

Confined phase.
Unique ground state has $V_x = 1$, $V_y = 1$.
No topological order

g

This criterion can distinguish the phases when dynamical (or even gapless) matter fields are present

Symmetry-enriched topological (SET) order and deconfined criticality

$$H = -\sum_{\square} \tau^z \tau^z \tau^z \tau^z - g \sum_i \tau^x \quad , \quad \boxed{G_i = -1}$$

Symmetry-enriched topological (SET) order and deconfined criticality

$$H = -\sum_{\square} \tau^z \tau^z \tau^z \tau^z - g \sum_i \tau^x \quad , \quad G_i = -1$$

Deconfined quantum criticality with a U(1) gauge theory

Deconfined phase.
4-fold degenerate ground state: $V_x = \pm 1$, $V_y = \pm 1$.
Can take linear combinations to make eigenstates with $W_x = \pm 1$, $W_y = \pm 1$.
Topological order

Confined phase.
Broken symmetry and valence bond solid (VBS) order

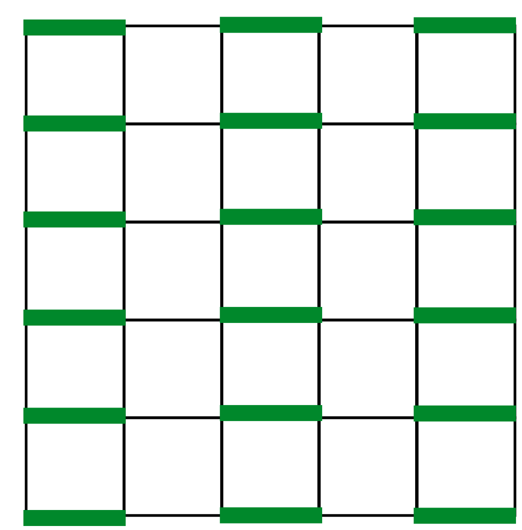

g

(R. Jalabert and S.S., 1991; T. Senthil, A. Vishwanath, L. Balents, S. S. and M.P.A. Fisher, 2004)

1. Z_2 lattice gauge theory and topological order

2. CP^1 theory of square lattice antiferromagnets and Z_2 topological order

3. Z_2 topological order and the volume enclosed by the Fermi surface

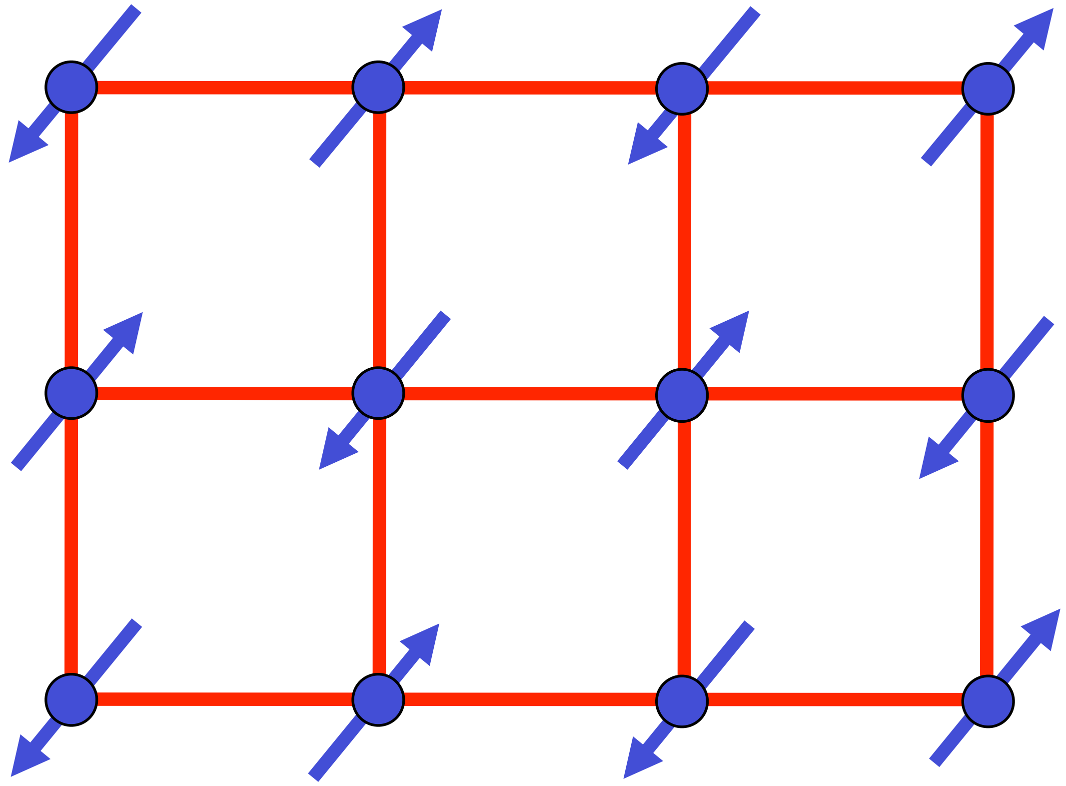

Insulating Antiferromagnet

Néel order parameter $\mathbf{n}(x_i, \tau) = \eta_i \mathbf{S}_i(\tau)$, where $\eta_i = \pm 1$ on two sublattices.
O(3) non-linear sigma model:

$$S = \frac{1}{2g} \int d^2 x d\tau \, (\partial_\mu \mathbf{n})^2$$

$\mathbb{CP}^1$ model: use $\mathbf{n} = z_\alpha^* \vec{\sigma}_{\alpha\beta} z_\beta$ with $\alpha, \beta = \uparrow, \downarrow$, and then

$$S = \frac{1}{g} \int d^2 x d\tau \, \left| (\partial_\mu - i a_\mu) z_\alpha \right|^2$$

where a_μ is an emergent U(1) gauge field.

Theory for $S = 1/2$ antiferromagnet also has spin Berry phase terms

$$S = \frac{1}{g} \int d^2 x d\tau \left| (\partial_\mu - i a_\mu) z_\alpha \right|^2 + i \sum_i \int d\tau \, \eta_i a_{i\tau}$$

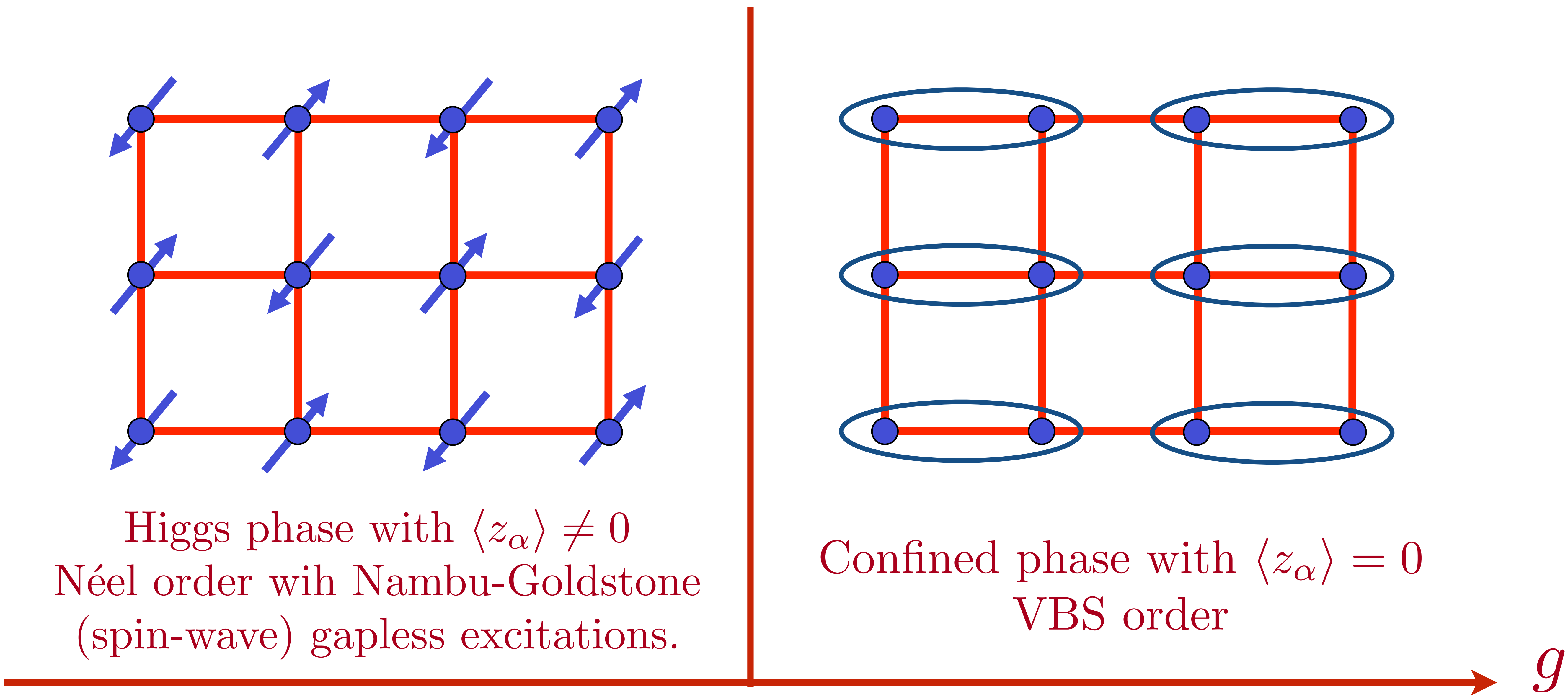

(N. Read and S.S., 1989; S.S. and R. Jalabert, 1990)

Theory for $S = 1/2$ antiferromagnet also has spin Berry phase terms

$$S = \frac{1}{g}\int d^2x d\tau \left|(\partial_\mu - i a_\mu) z_\alpha\right|^2 + i \sum_i \int d\tau\, \eta_i a_{i\tau}$$

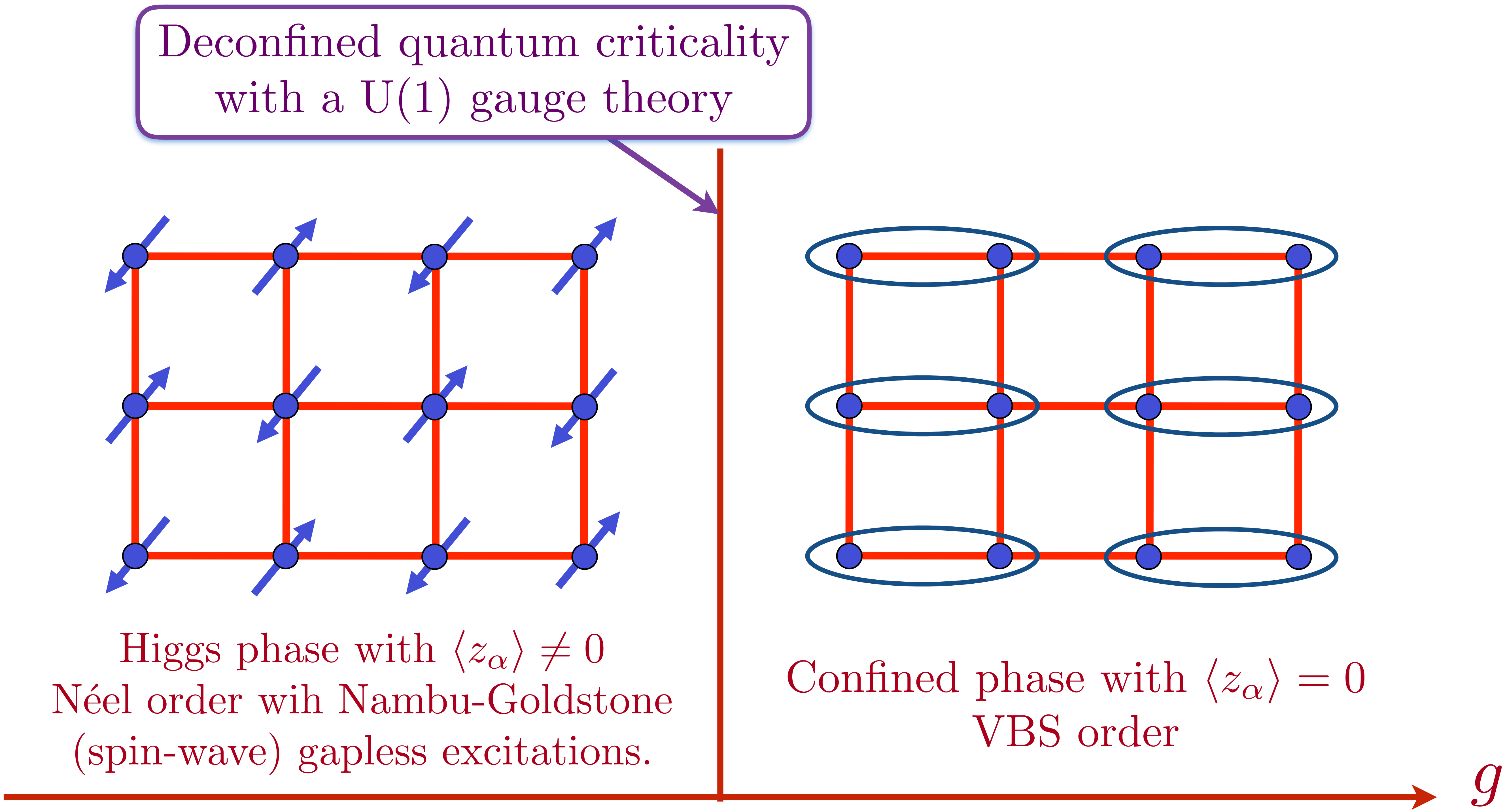

(T. Senthil, A. Vishwanath, L. Balents, S. S. and M.P.A. Fisher, 2004)

To obtain a Z_2 deconfined phase, we need to condense a Higgs field, Φ, with U(1) charge 2.

(Fradkin and Shenker, 1979)

The phase of Φ winds by 2π around the cycle of the torus, trapping U(1) flux π in the hole of the torus. This leads to 4-fold ground state degeneracy

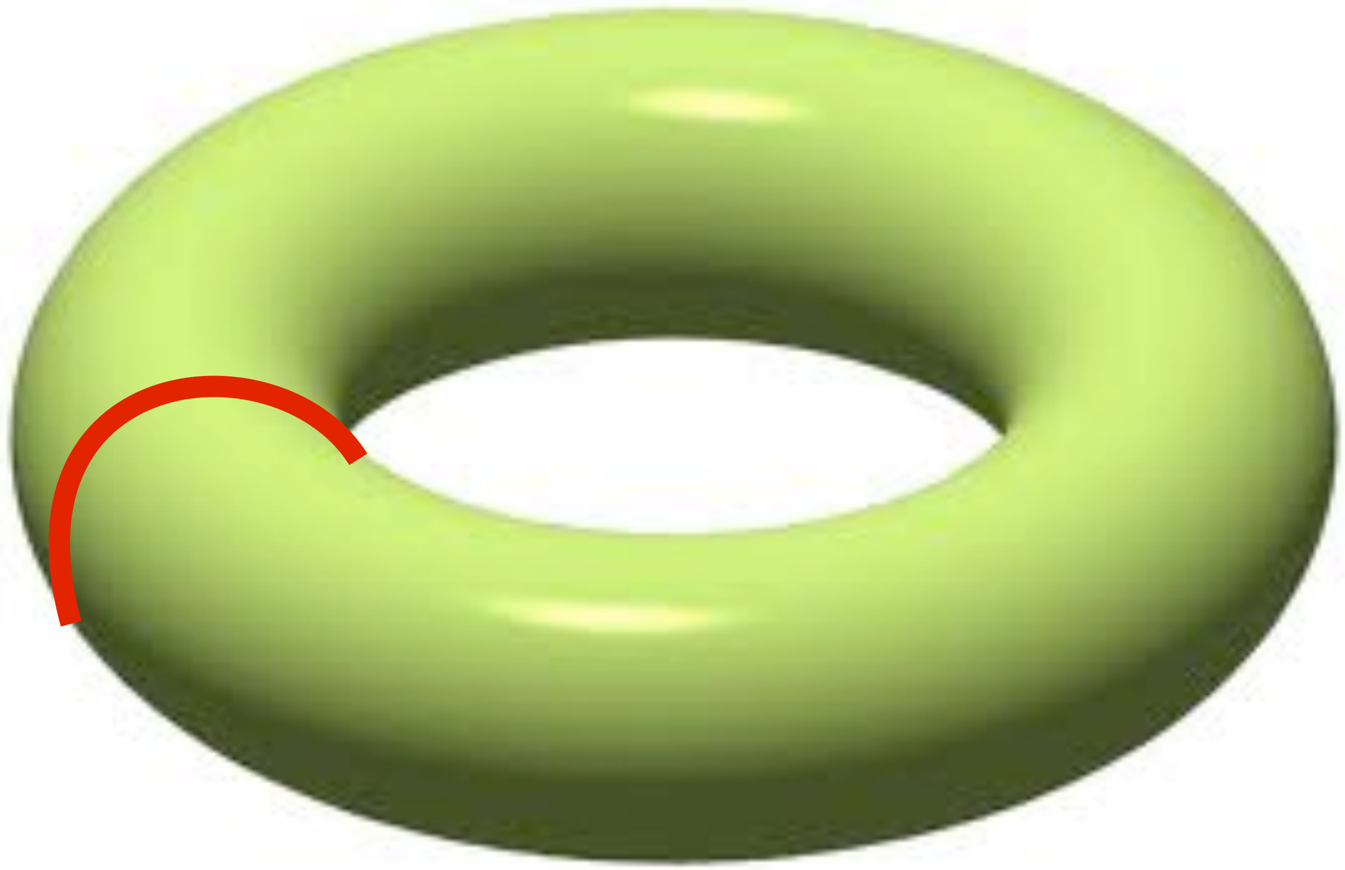

(N. Read and S.S., 1991; X.G.Wen, 1991)

The simplest route to such Higgs fields is to condense spin-singlet pairs of long-wavelength spinons, z_α. There are two candidates for such Higgs fields, corresponding to the operators

$$\varepsilon_{\alpha\beta} z_\alpha \partial_\tau z_\beta \quad , \quad \varepsilon_{\alpha\beta} z_\alpha \vec{\nabla} z_\beta$$

So we introduce corresponding Higgs fields, P and $\vec{Q}$, and the following effective action with additional tuning parameters s_1 and s_2

$$S = \frac{1}{g} \int d^2x d\tau \, |(\partial_\mu - i a_\mu) z_\alpha|^2 + i \sum_i \int d\tau \, \eta_i a_{i\tau}$$
$$\int d^2x d\tau \Big[iP \, \varepsilon_{\alpha\beta} z_\alpha \partial_\tau z_\beta + \vec{Q} \cdot \varepsilon_{\alpha\beta} z_\alpha \vec{\nabla} z_\beta + \text{H.c.}$$
$$+ s_1 |P|^2 + s_2 |\vec{Q}|^2 + u_1 |P|^4 + u_2 |\vec{Q}|^4 + \ldots \Big]$$

Phase diagram at large g with $\langle z_\alpha \rangle = 0$

Three phases with Z_2 topological order

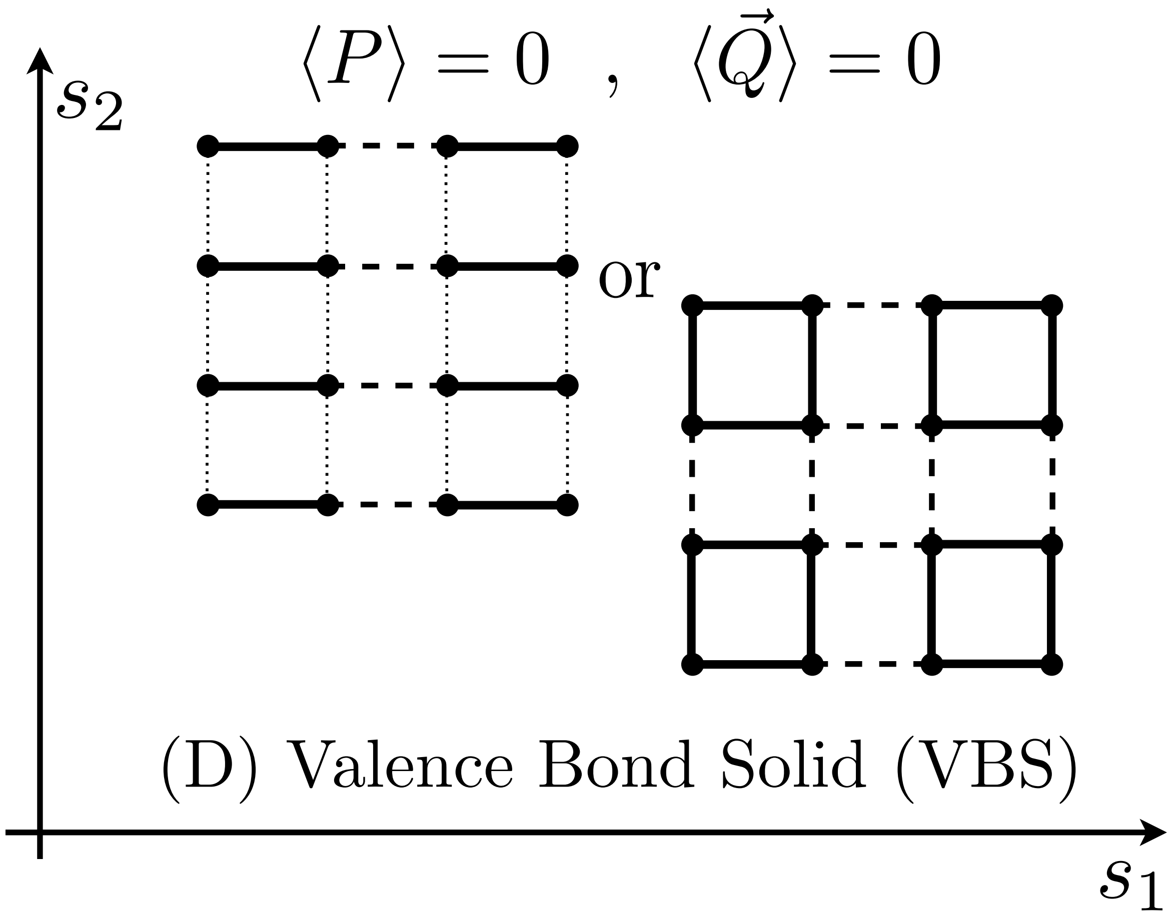

Phase diagram at large g with $\langle z_\alpha \rangle = 0$

Three phases with Z_2 topological order

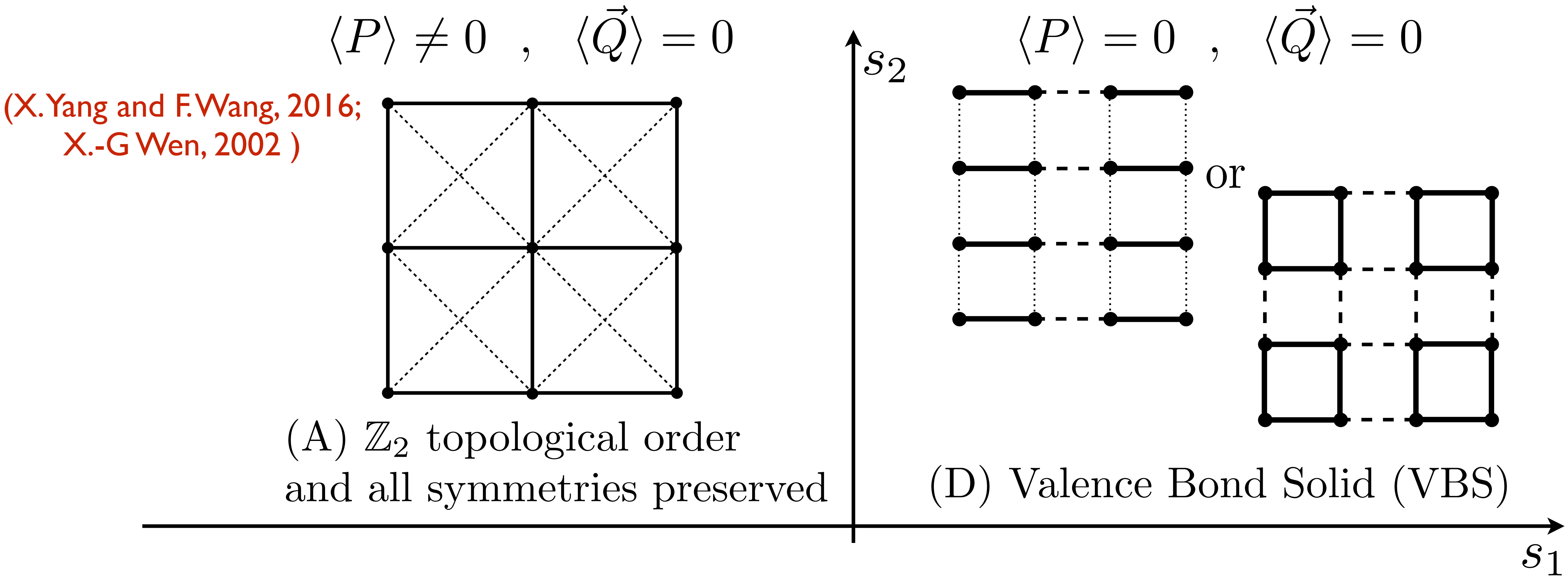

Phase diagram at large g with $\langle z_\alpha \rangle = 0$

Three phases with Z_2 topological order

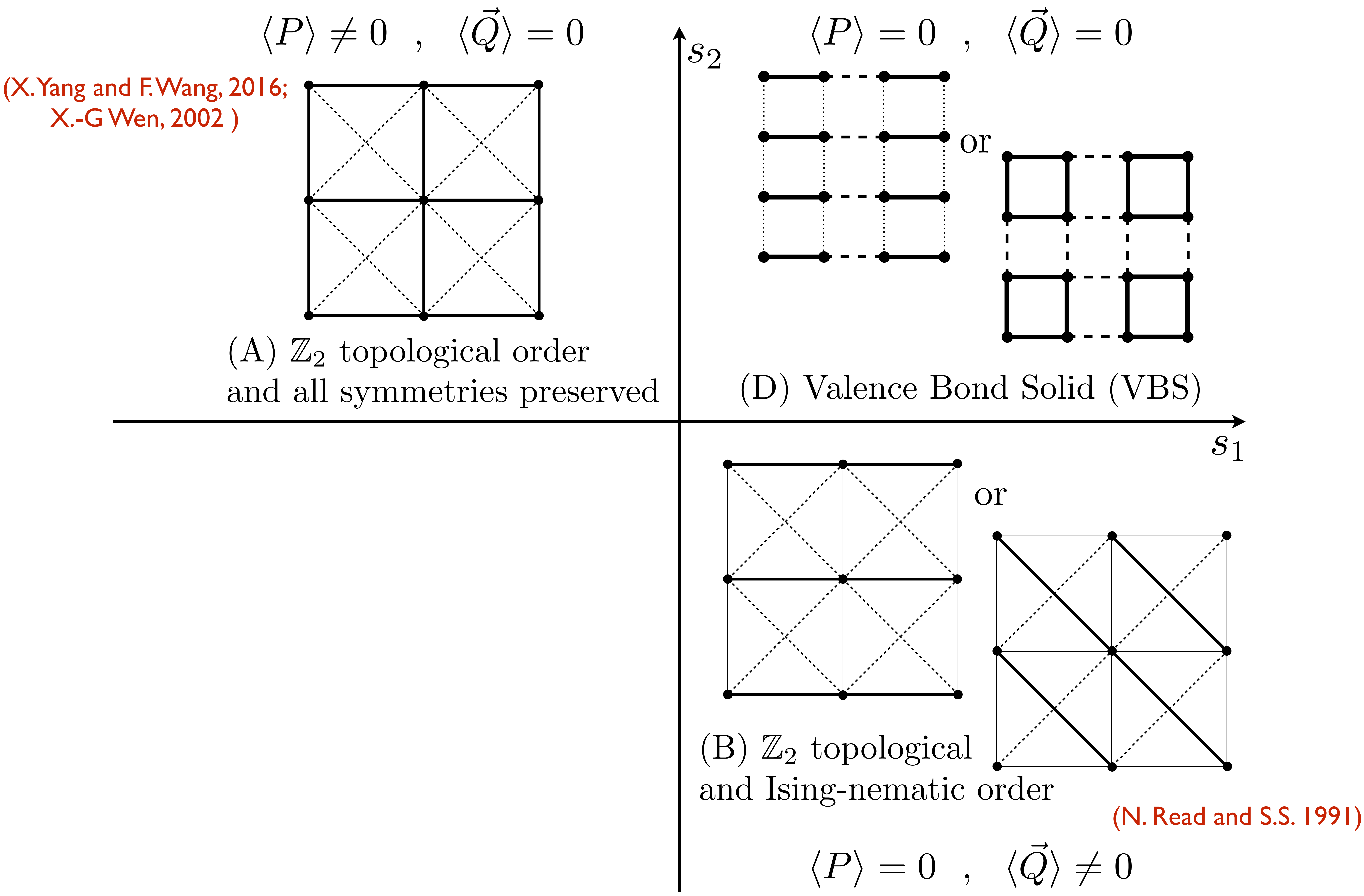

Phase diagram at large g with $\langle z_\alpha \rangle = 0$

Three phases with Z_2 topological order

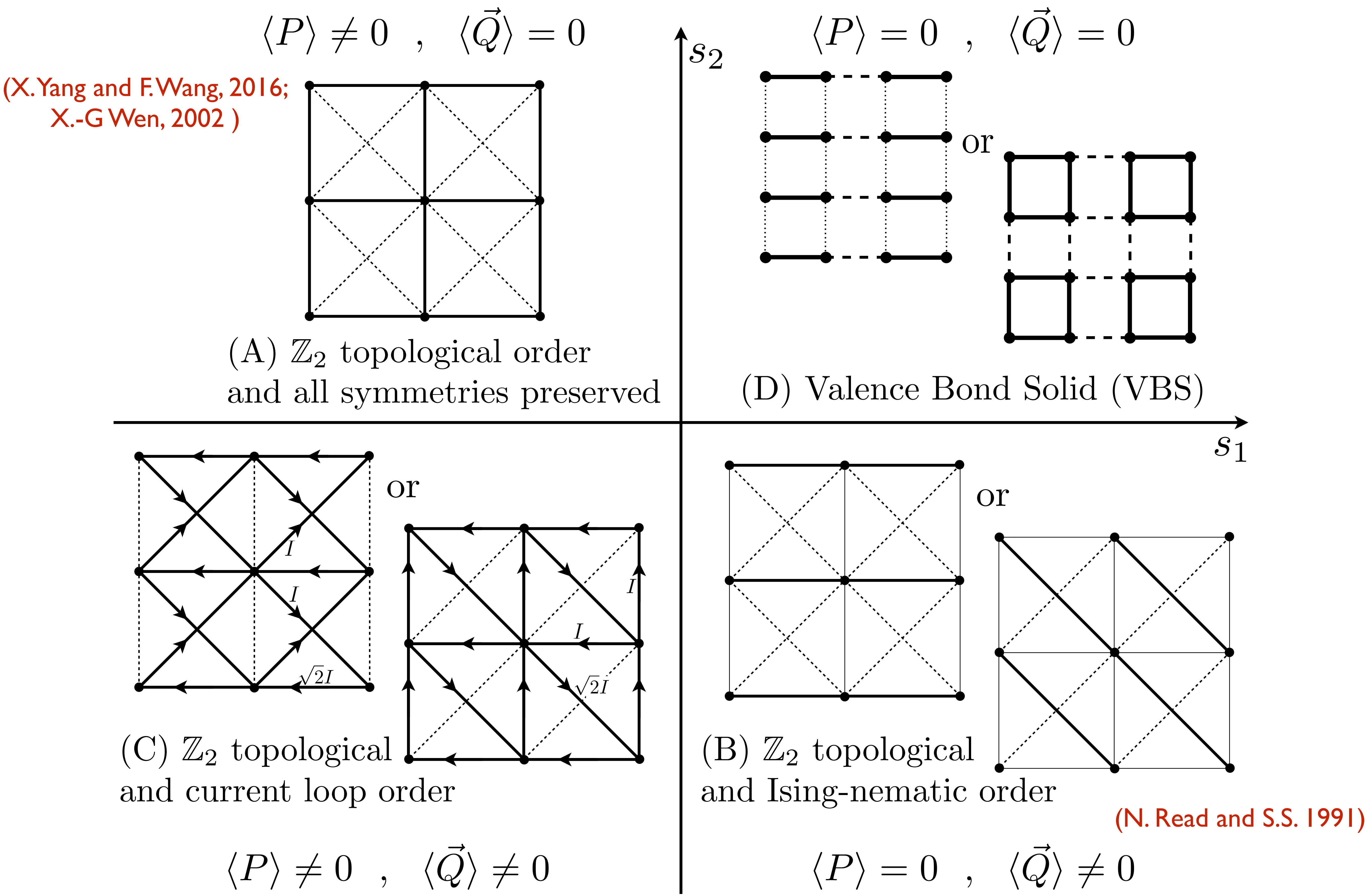

Phase diagram at large g with $\langle z_\alpha \rangle = 0$

Three phases with Z_2 topological order

s_2

$\langle P \rangle \neq 0 \;,\; \langle \vec{Q} \rangle = 0$

(X. Yang and F. Wang, 2016; X.-G Wen, 2002)

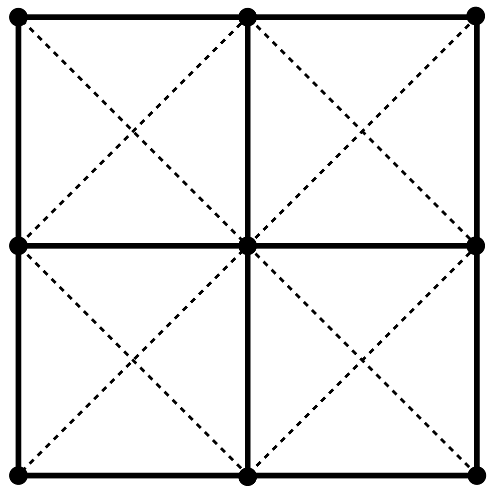

(A) $\mathbb{Z}_2$ topological order and all symmetries preserved

$\langle P \rangle = 0 \;,\; \langle \vec{Q} \rangle = 0$

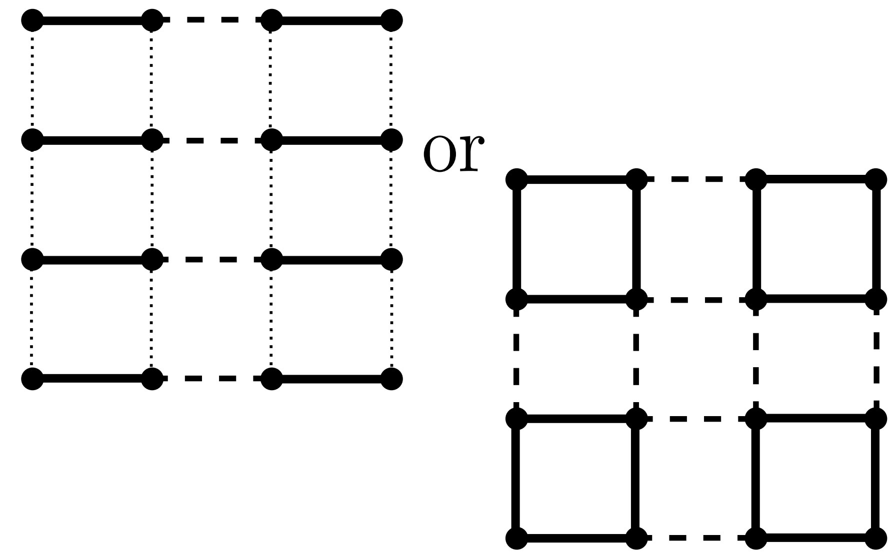

(D) Valence Bond Solid (VBS)

The broken symmetries co-existing with Z_2 topological order are precisely those observed in the pseudogap phase of the cuprates

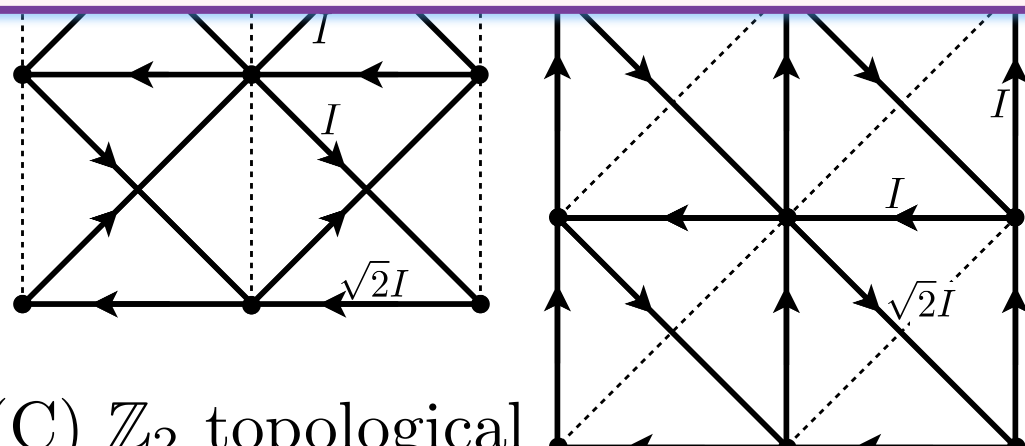

(C) $\mathbb{Z}_2$ topological and current loop order

$\langle P \rangle \neq 0 \;,\; \langle \vec{Q} \rangle \neq 0$

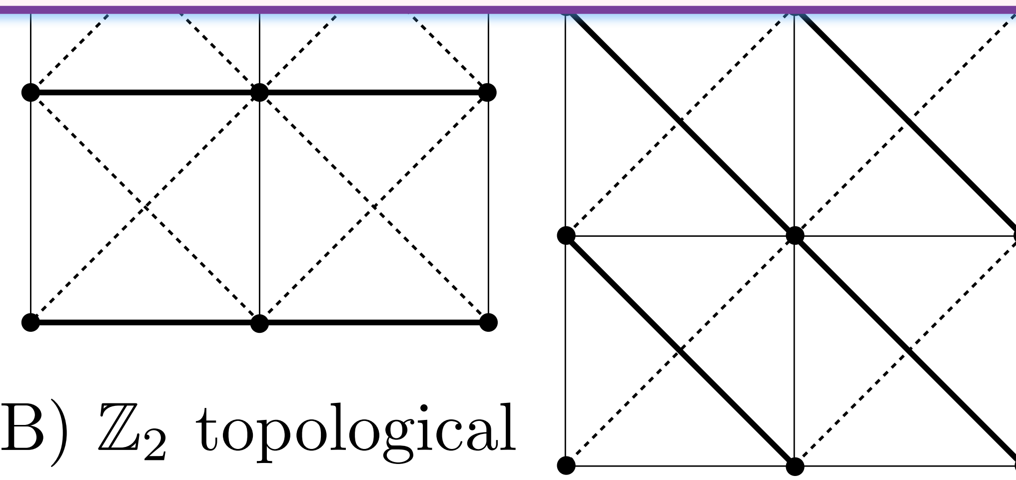

(B) $\mathbb{Z}_2$ topological and Ising-nematic order

(N. Read and S.S. 1991)

$\langle P \rangle = 0 \;,\; \langle \vec{Q} \rangle \neq 0$

Broken inversion symmetry below T^* in $YBa_2Cu_3O_y$

No anomalies at T_c, T_{CDW} or T_{Kerr}

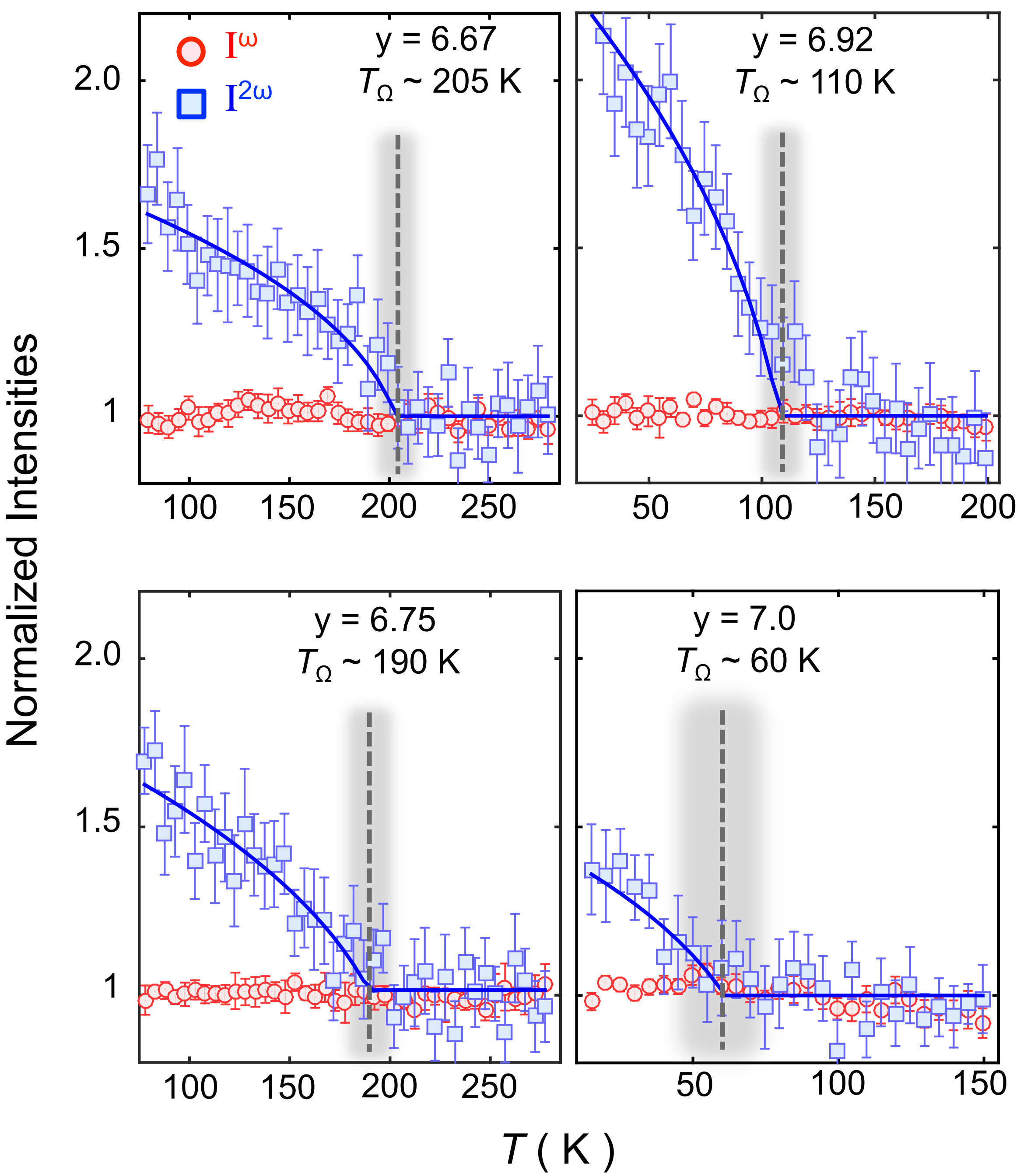

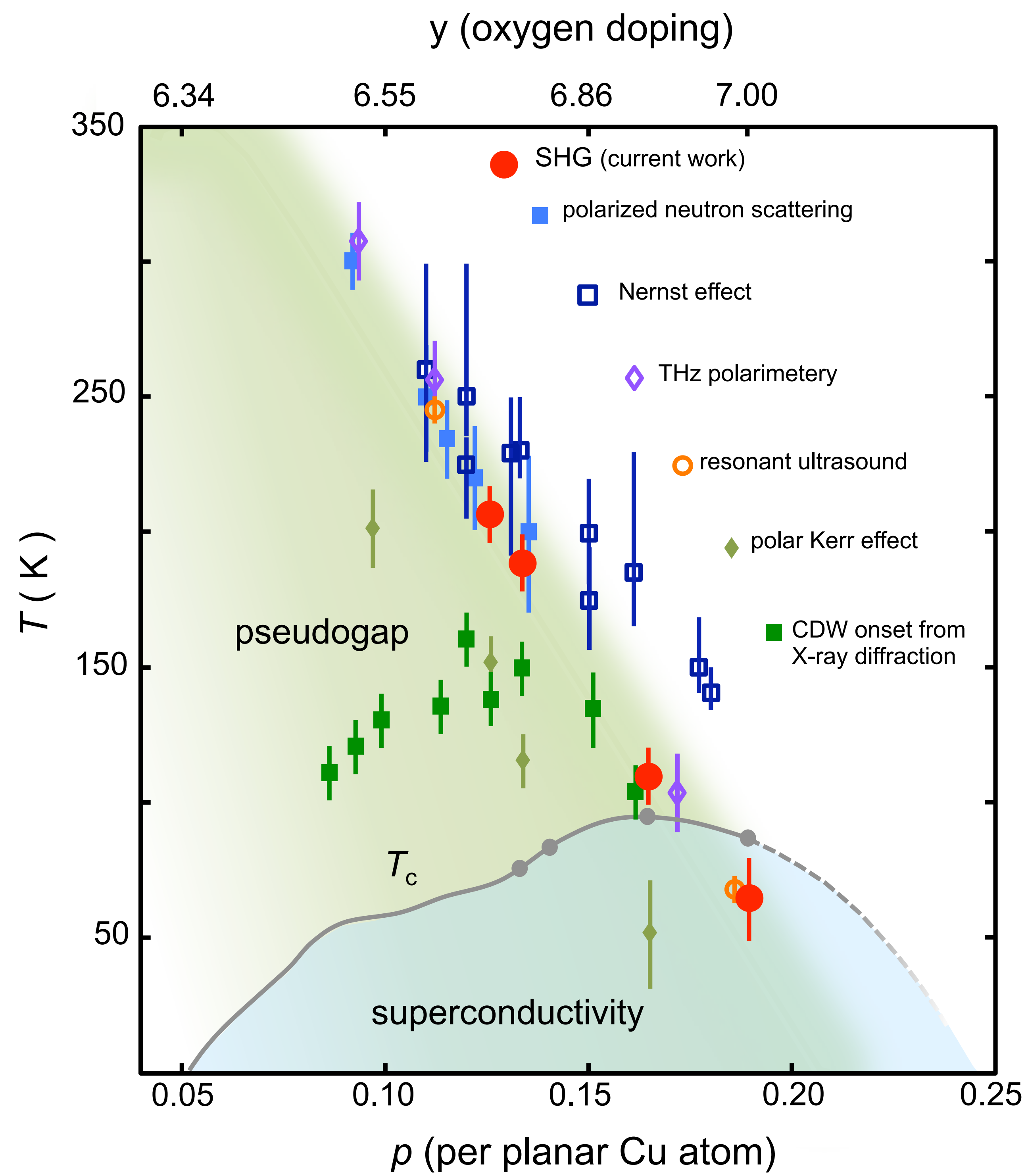

L. Zhao, C.A. Belvin, R. Liang, D.A. Bonn, W. N. Hardy, N. P. Armitage, and D. Hsieh, Nature Physics **13**, 250 (2017)

Phase diagram of $Sr_2Ir_{1-x}Rh_xO_4$

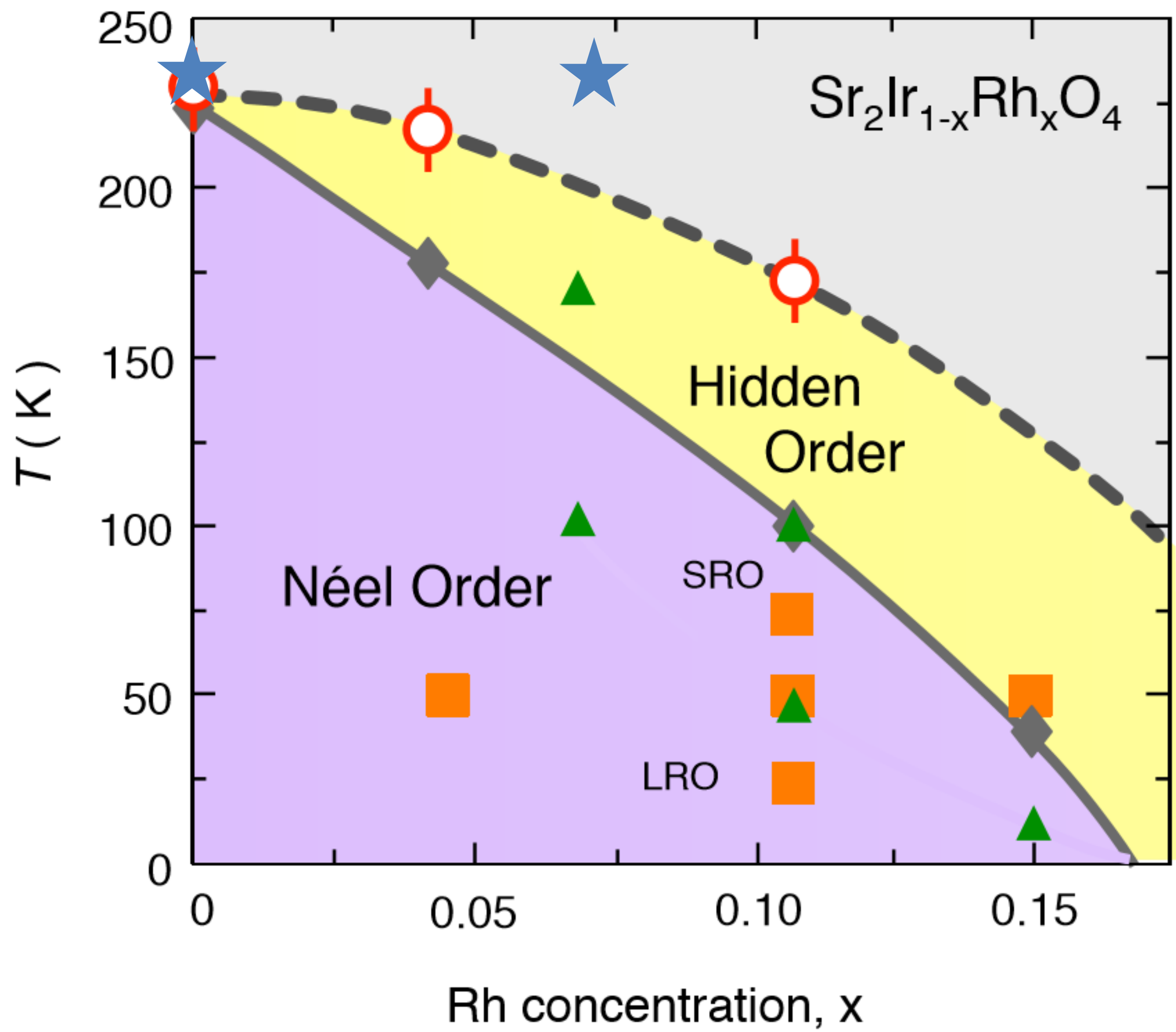

SHG (T_Ω)

DC magnetic susceptibility (T_N)

T. Qi *et al.*, PRB 86, 125105 (2012)

Resonant x-ray diffraction (T_N)

J. P. Clancy *et al.*, PRB 89, 054409 (2014)

ARPES (pseudogap present)

Y. Cao *et al.*, Nat. Commun. 7, 11367 (2016)

Polarized neutron diffraction

J. Jeong *et al.*, arXiv:1701.06485 (2017)

L. Zhao, D. H. Torchinsky, H. Chu, V. Ivanov, R. Lifshitz, R. Flint, T. Qi, G. Cao, and D. Hsieh, Nature Physics **12**, 32 (2016)

Phase diagram at large g with $\langle z_\alpha \rangle = 0$

Three phases with Z_2 topological order

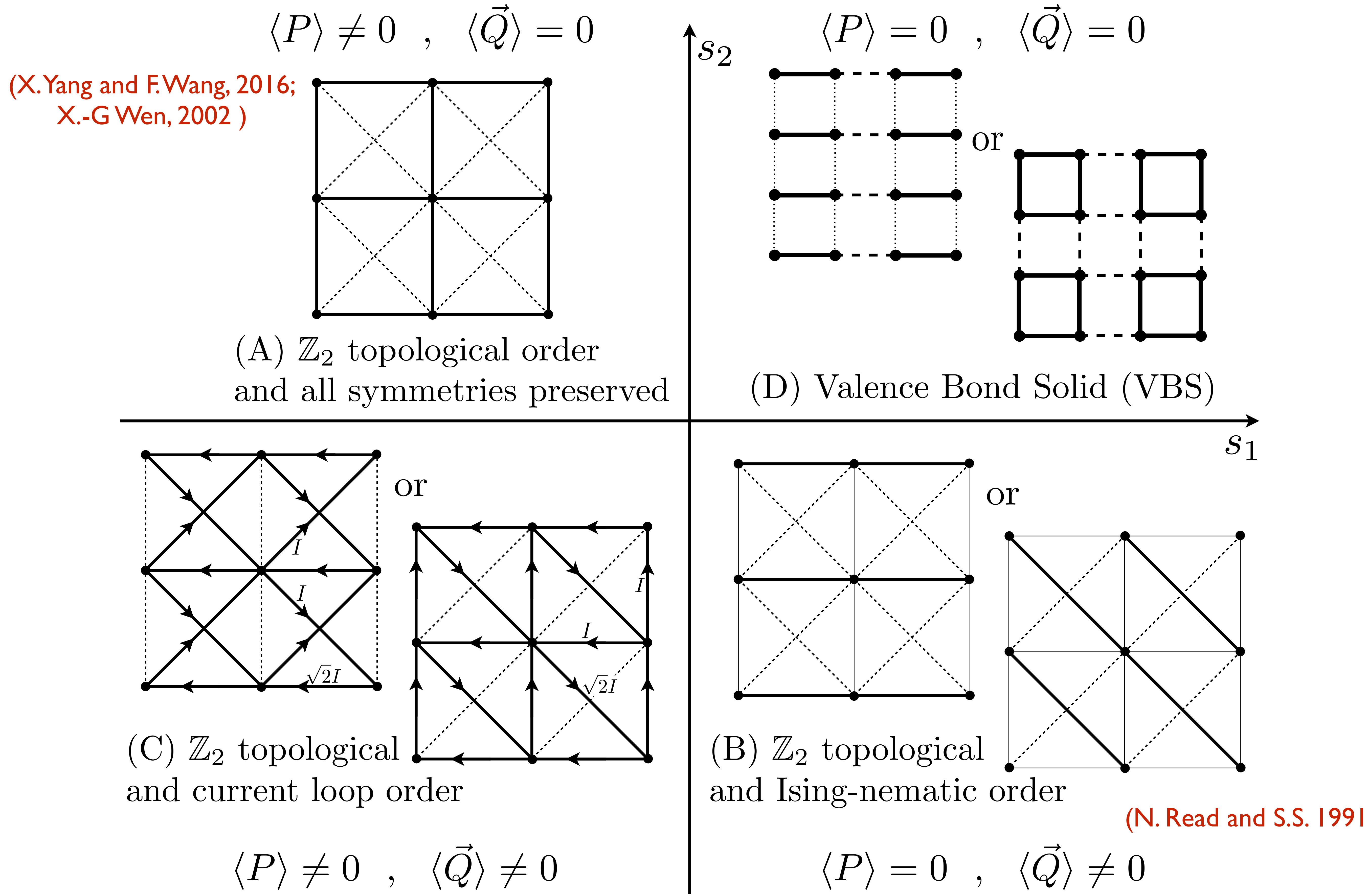

Phase diagram at small g with $\langle z_\alpha \rangle \neq 0$

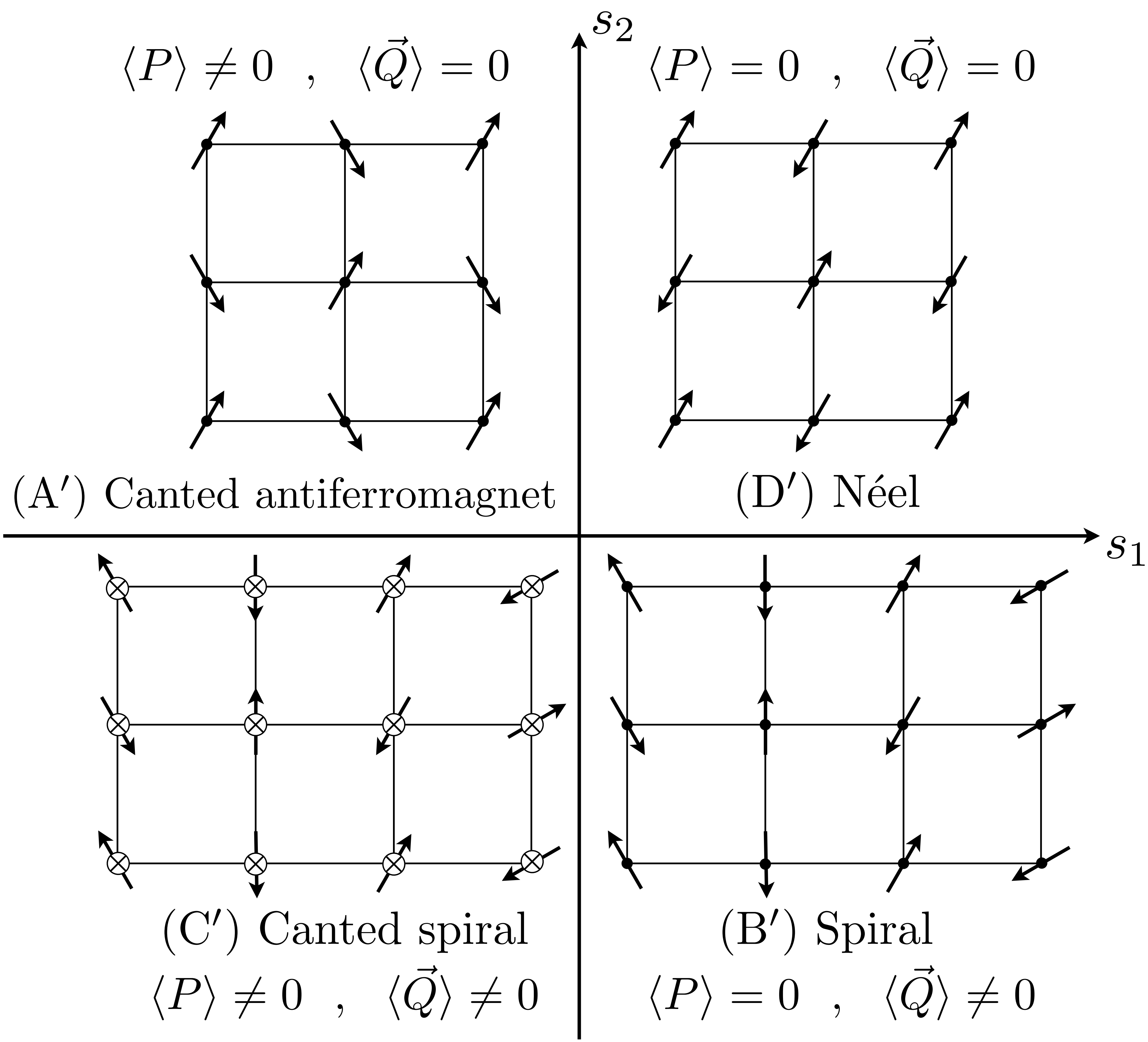

An attractive possibility at intermediate g with $\langle z_\alpha \rangle = 0$

s_2

s_1

$\langle P \rangle \neq 0$, $\langle \vec{Q} \rangle \neq 0$

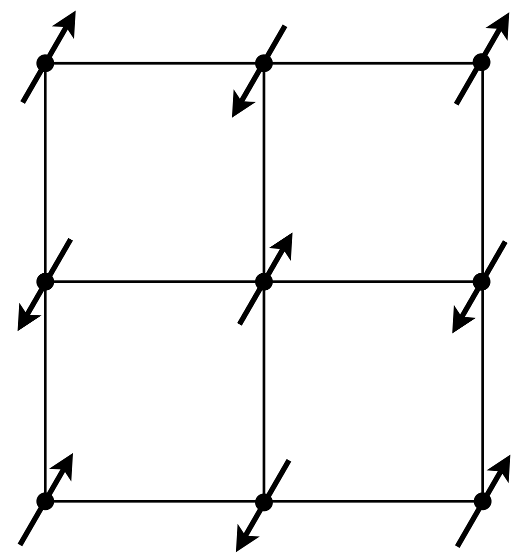

$$\left\langle z_\alpha^* \sigma^a_{\alpha\beta} z_\beta \right\rangle \neq 0$$

$$\langle z_\alpha \rangle = 0$$

The AF* state:

co-existing

$\mathbb{Z}_2$ topological

and Néel order.

Gapped $S = 1/2$ spinons

and gapless spin waves.

Fractional excitations in the square-lattice quantum antiferromagnet

B. Dalla Piazza, M. Mourigal, N. B. Christensen, G. J. Nilsen, P. Tregenna-Piggott, T. G. Perring, M. Enderle, D. F. McMorrow, D. A. Ivanov, and H. M. Rønnow,
Nature Physics 11, 62 (2015)

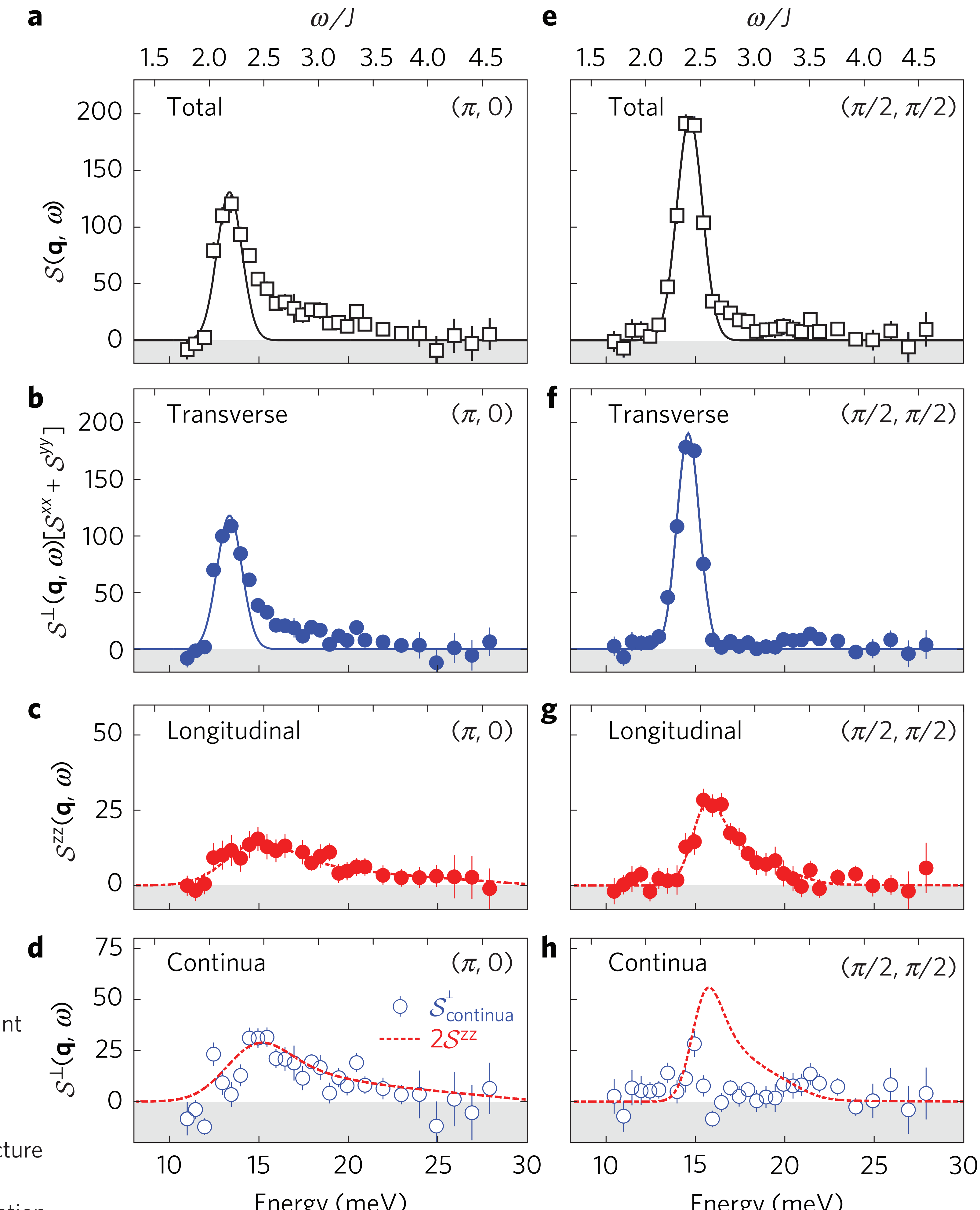

Figure 2 | Summary of the polarized neutron scattering data. **a–c**,**e–g**, Energy dependence of the total, transverse and longitudinal contributions to the dynamic structure factor, respectively, at constant wavevectors $\mathbf{q}=(\pi,0)$ (**a–c**) and $\mathbf{q}=(\pi/2,\pi/2)$ (**e–g**) measured by polarized neutron scattering on CFTD. The solid lines indicate resolution-limited Gaussian fits, while the dashed lines are empirical lineshapes used as guides-to-the-eye. **d**,**h**, Transverse dynamic structure factor with subtracted resolution-limited Gaussian fits at $(\pi,0)$ and $(\pi/2,\pi/2)$, respectively. Error bars correspond to one standard deviation.

1. Z_2 lattice gauge theory and topological order

2. CP^1 theory of square lattice antiferromagnets and Z_2 topological order

3. Z_2 topological order and the volume enclosed by the Fermi surface

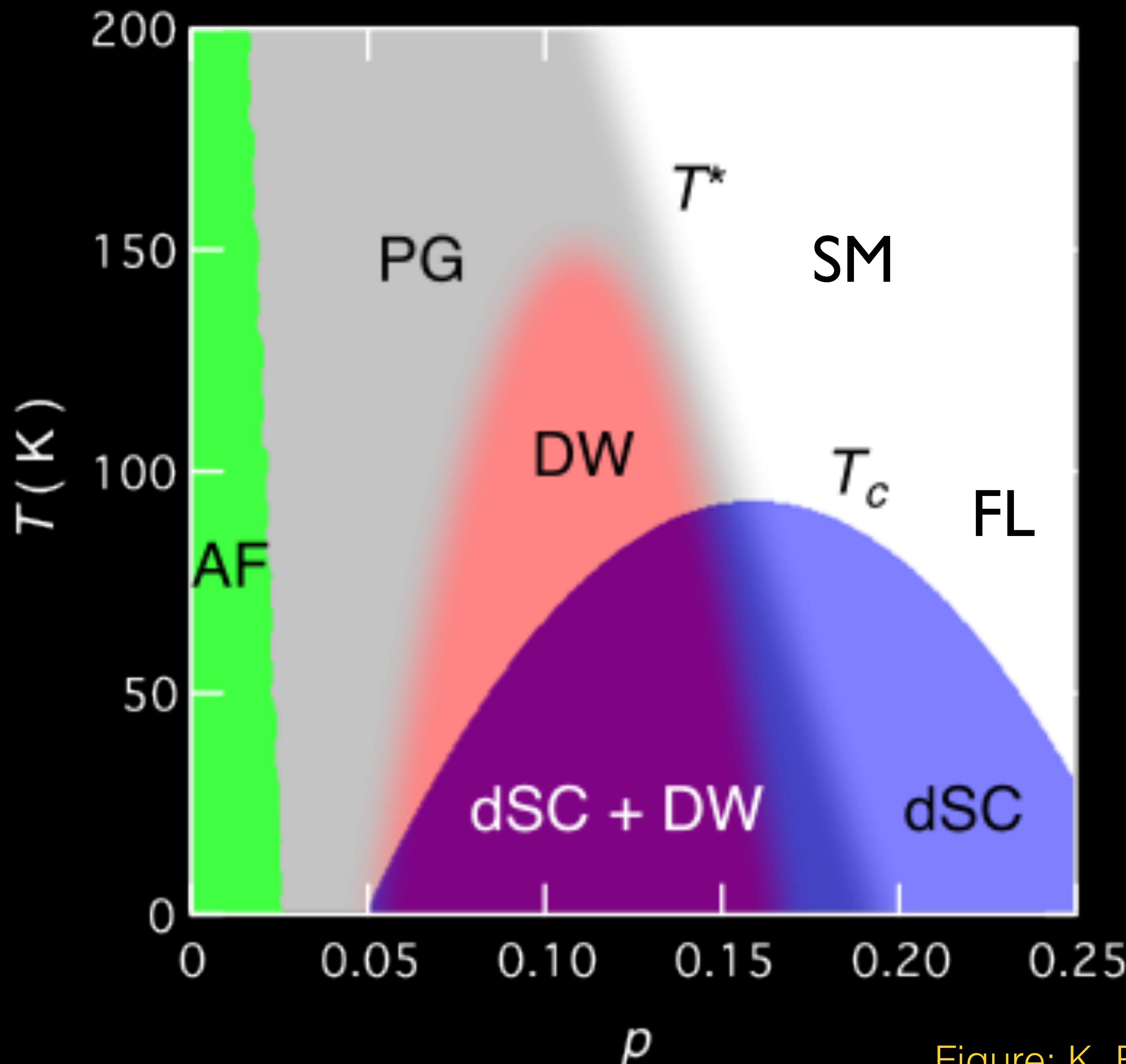

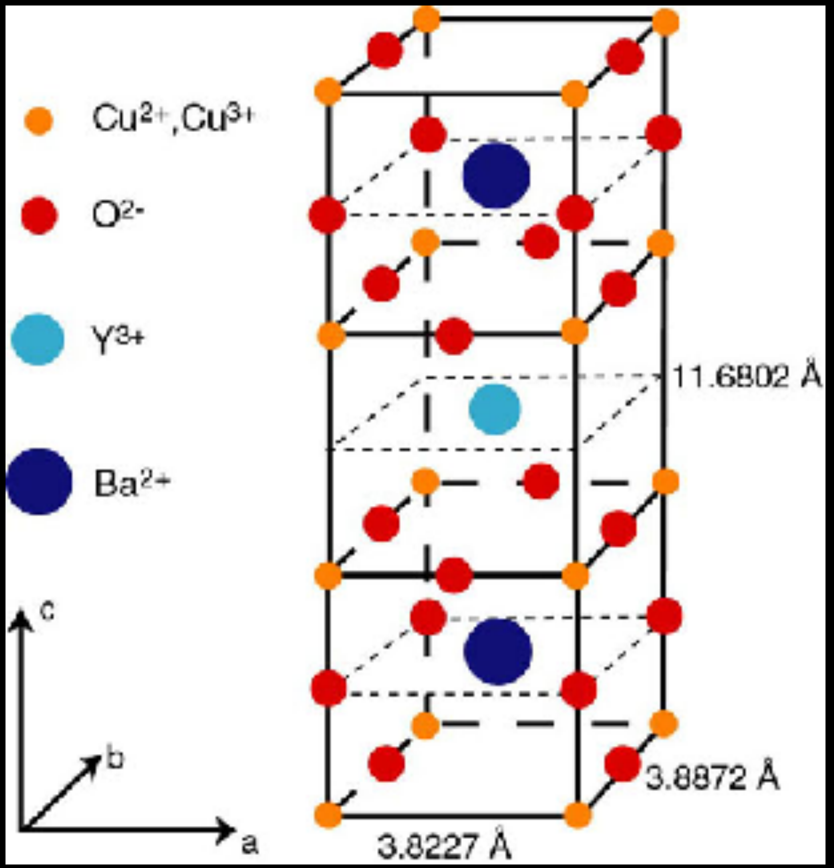

$YBa_2Cu_3O_{6+x}$

Figure: K. Fujita and J. C. Seamus Davis

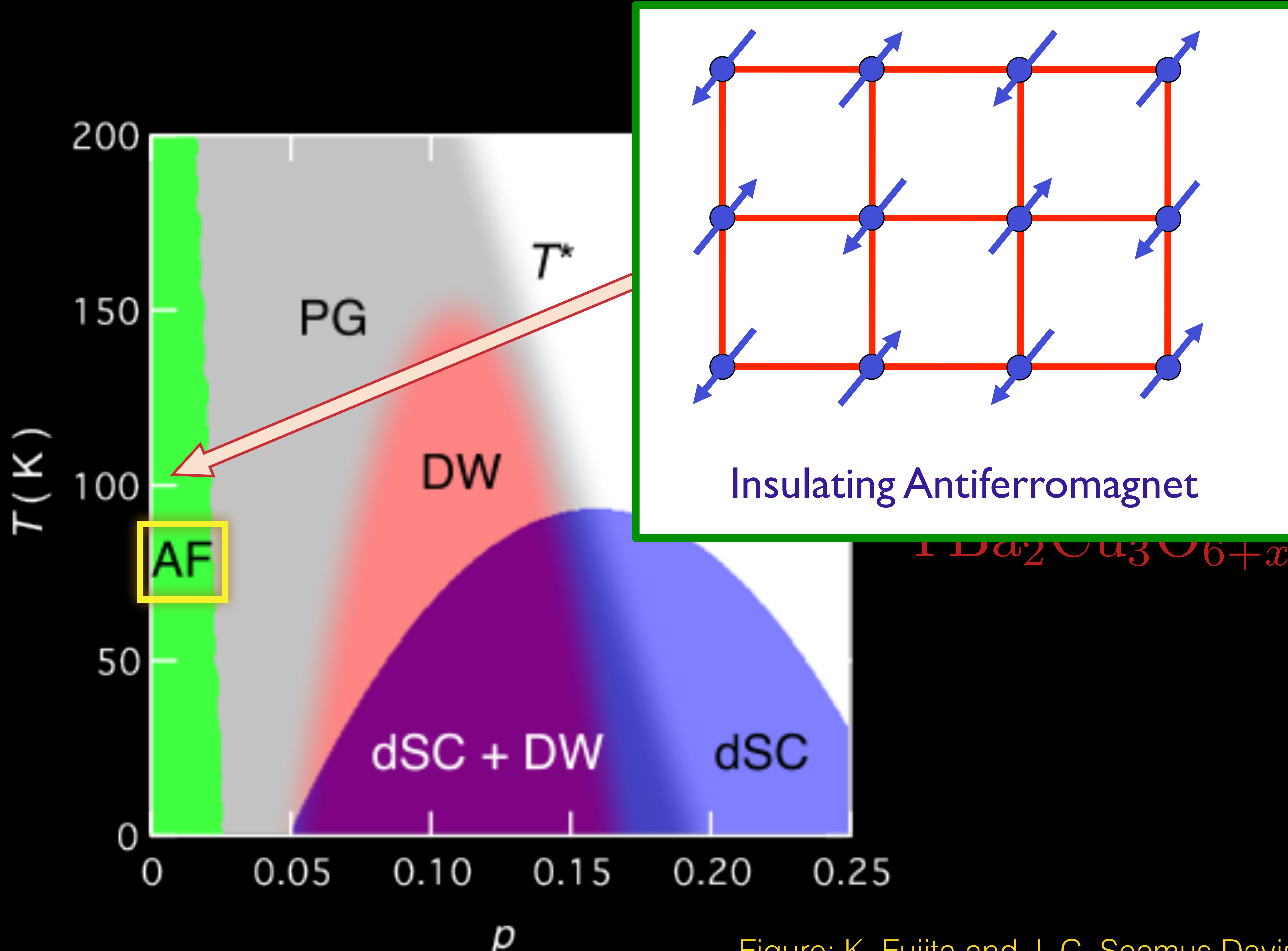

Figure: K. Fujita and J. C. Seamus Davis

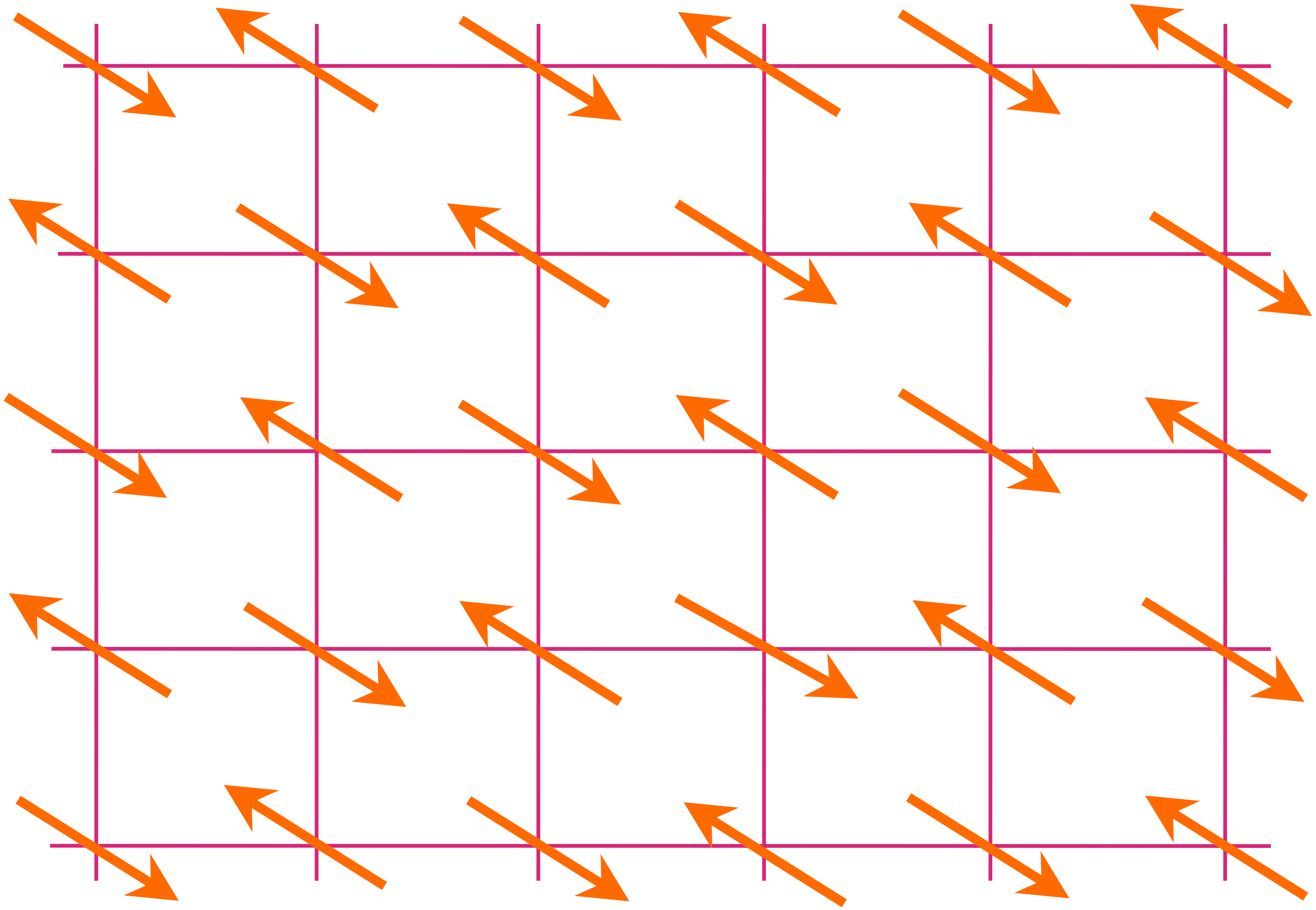

"Undoped" insulating anti-ferromagnet

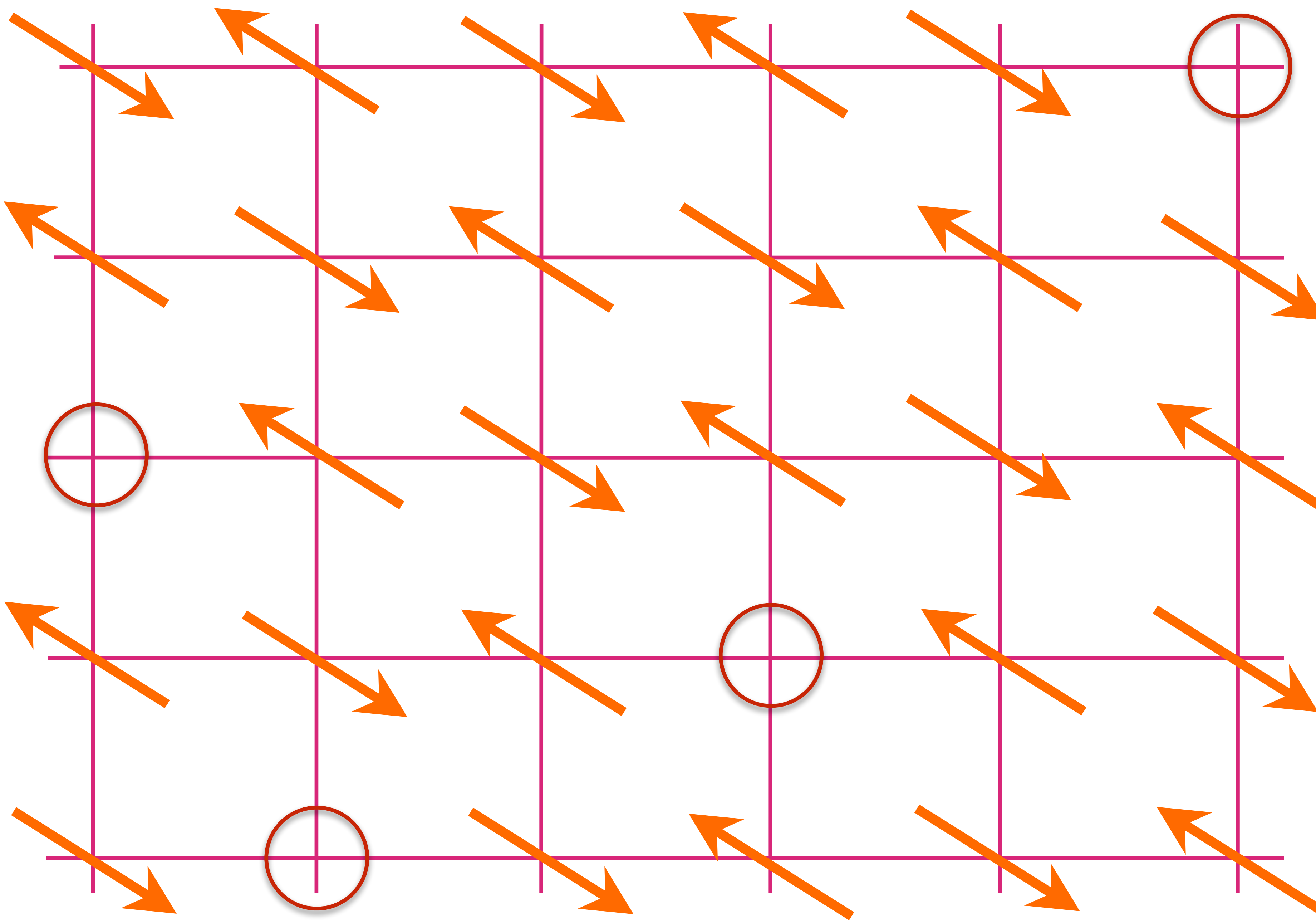

Anti-
ferromagnet
with p mobile
holes
per square

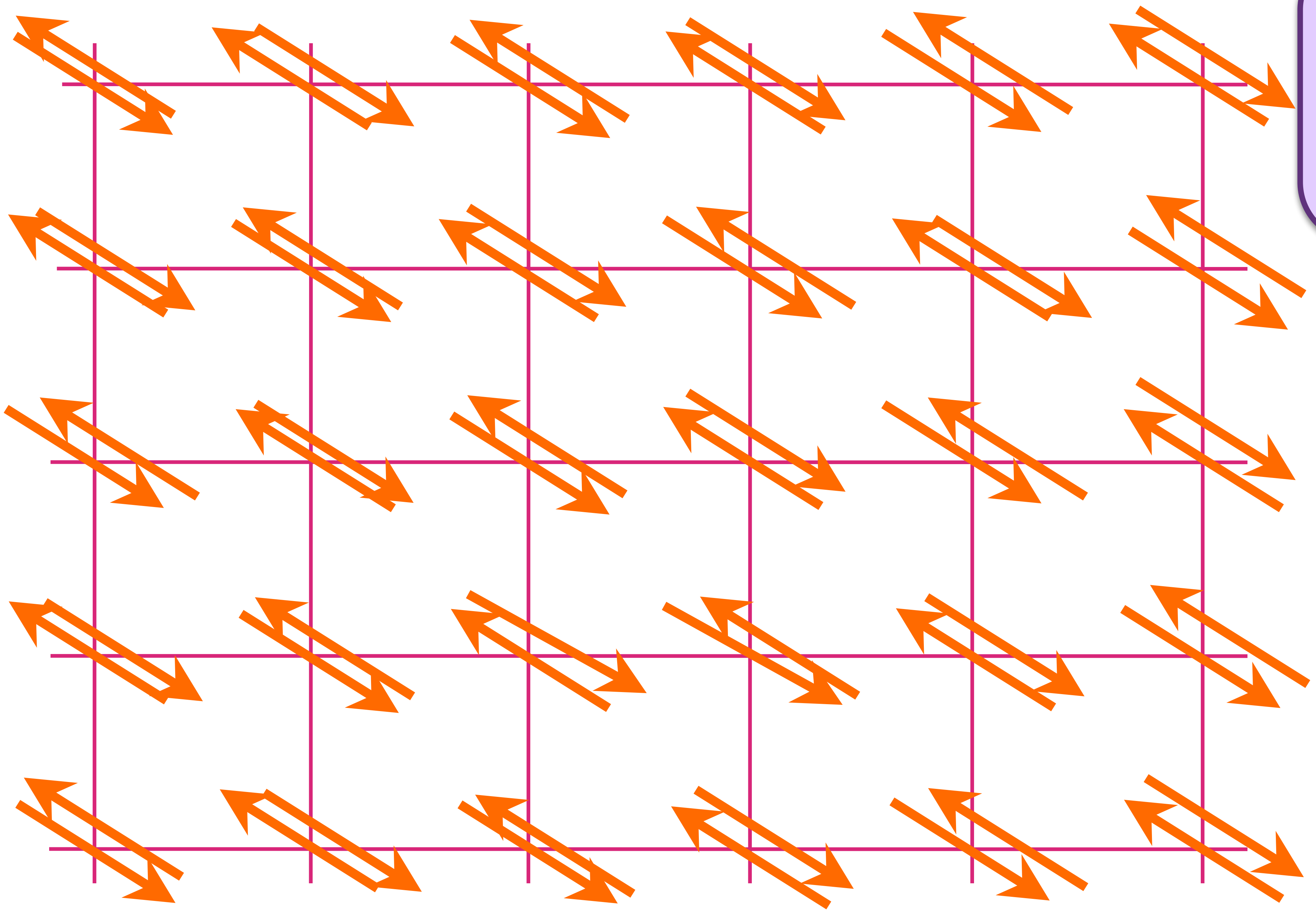

Filled Band

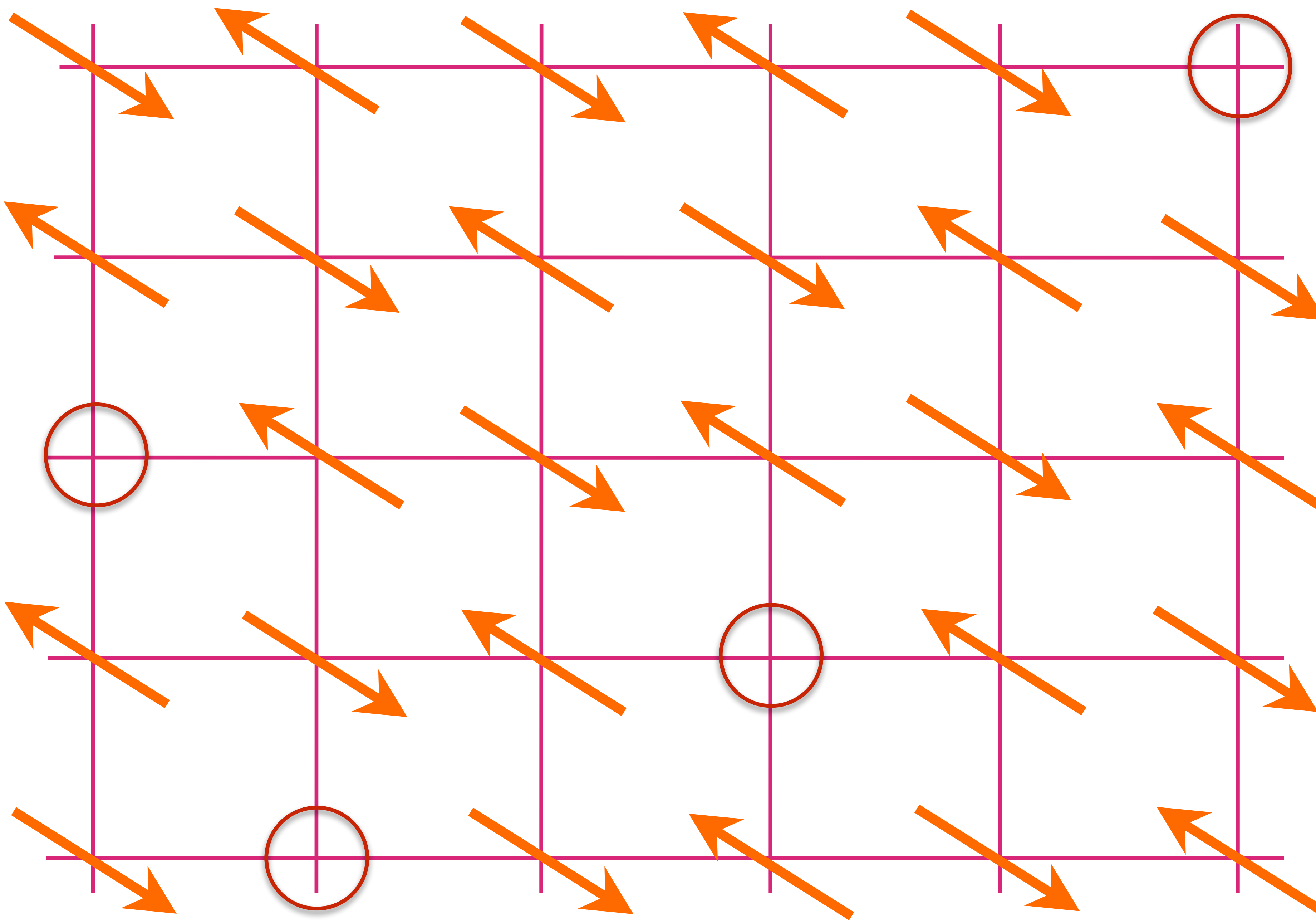

Anti-ferromagnet with p mobile holes per square

But relative to the band insulator, there are $1+p$ holes per square

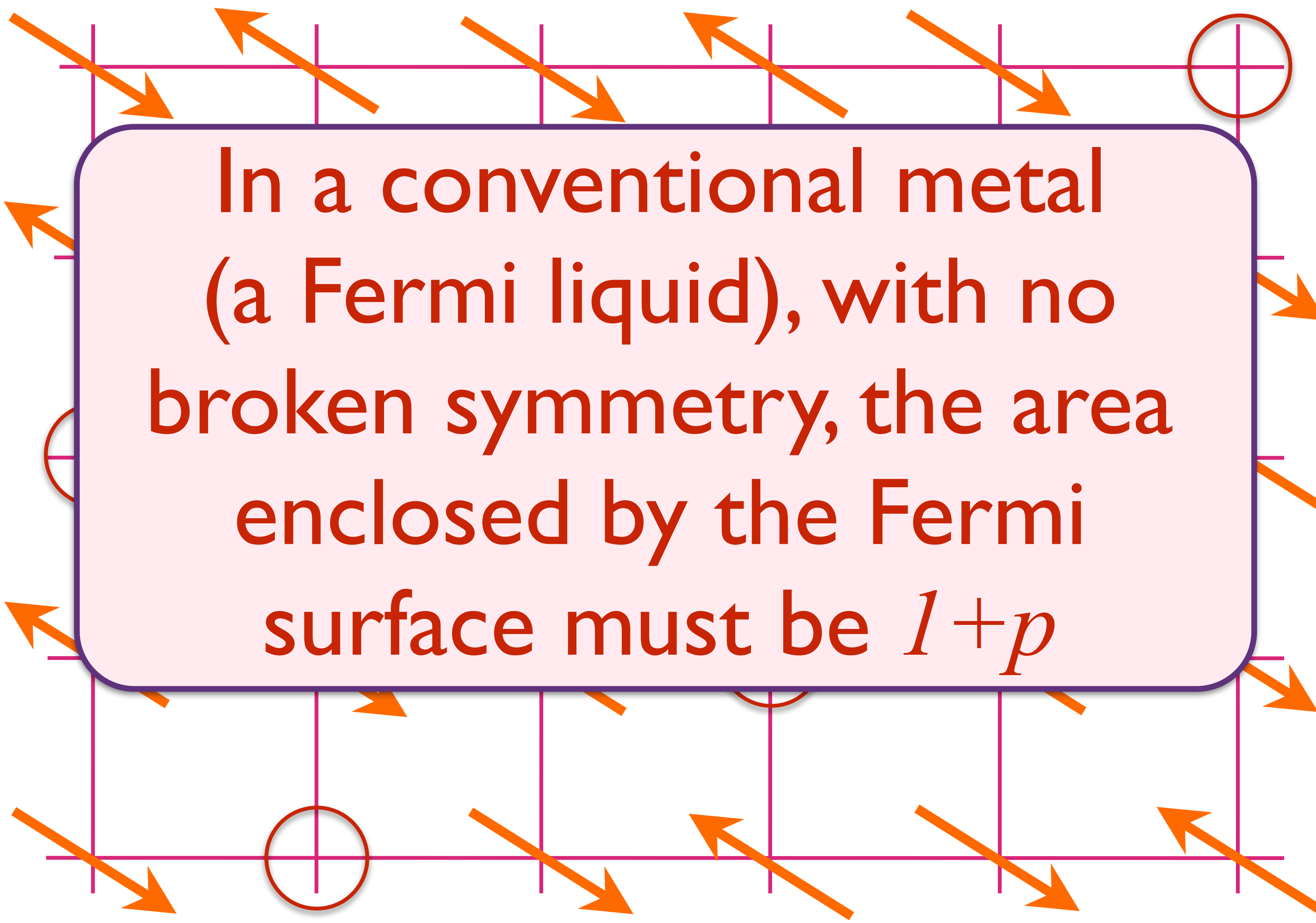

In a conventional metal (a Fermi liquid), with no broken symmetry, the area enclosed by the Fermi surface must be $1+p$

Anti-ferromagnet with p mobile holes per square

But relative to the band insulator, there are $1+p$ holes per square

M. Platé, J. D. F. Mottershead, I. S. Elfimov, D. C. Peets, Ruixing Liang, D. A. Bonn, W. N. Hardy, S. Chiuzbaian, M. Falub, M. Shi, L. Patthey, and A. Damascelli, Phys. Rev. Lett. **95**, 077001 (2005)

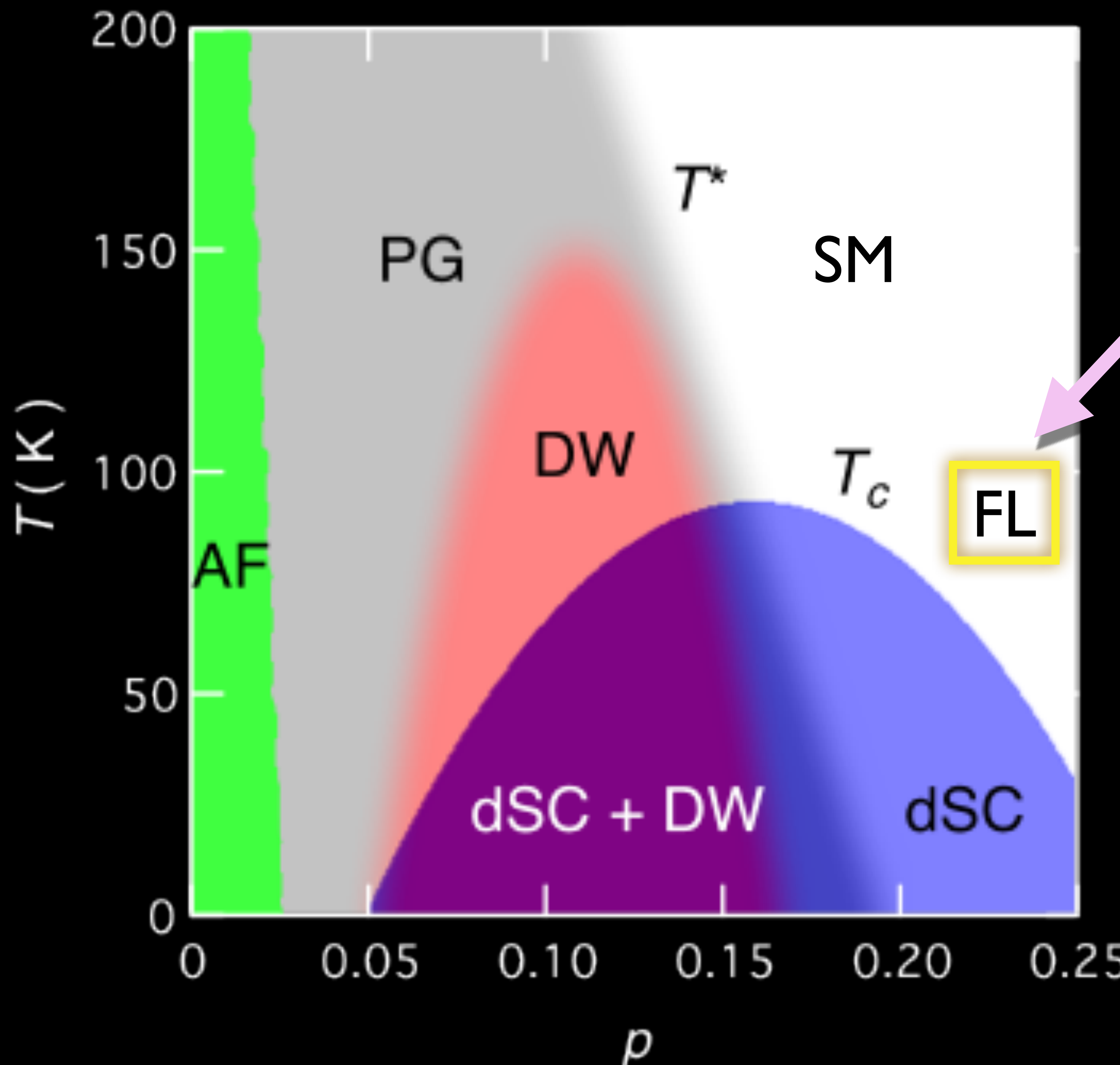

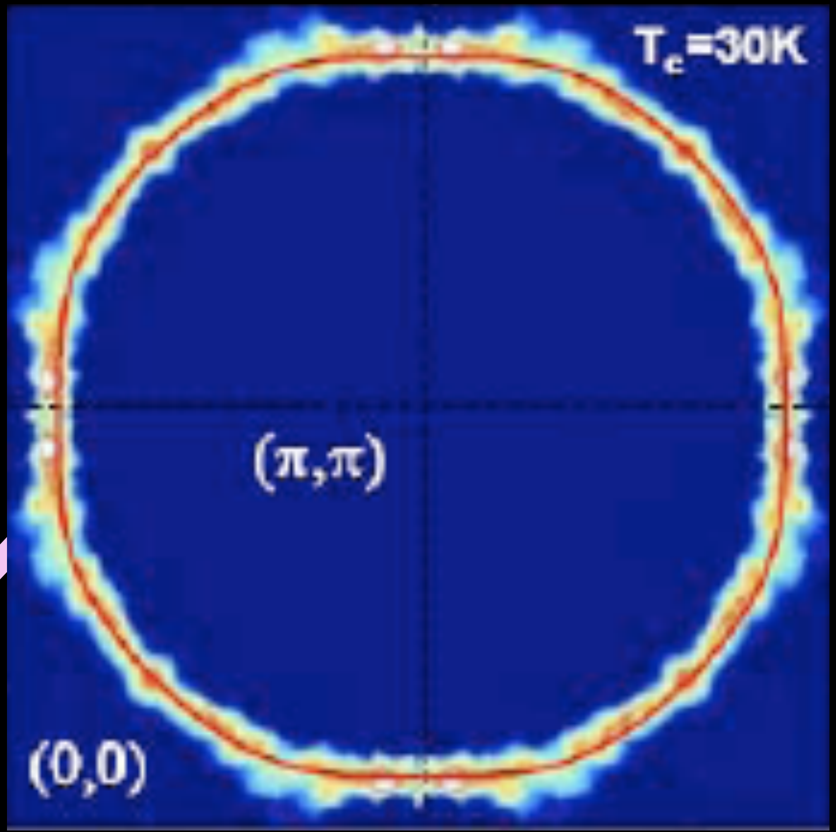

A conventional metal:
the Fermi liquid with Fermi surface of size *1+p*

S. Badoux, W. Tabis, F. Laliberté, G. Grissonnanche, B. Vignolle, D. Vignolles, J. Béard, D.A. Bonn, W.N. Hardy, R. Liang, N. Doiron-Leyraud, L. Taillefer, and C. Proust, Nature **531**, 210 (2016).

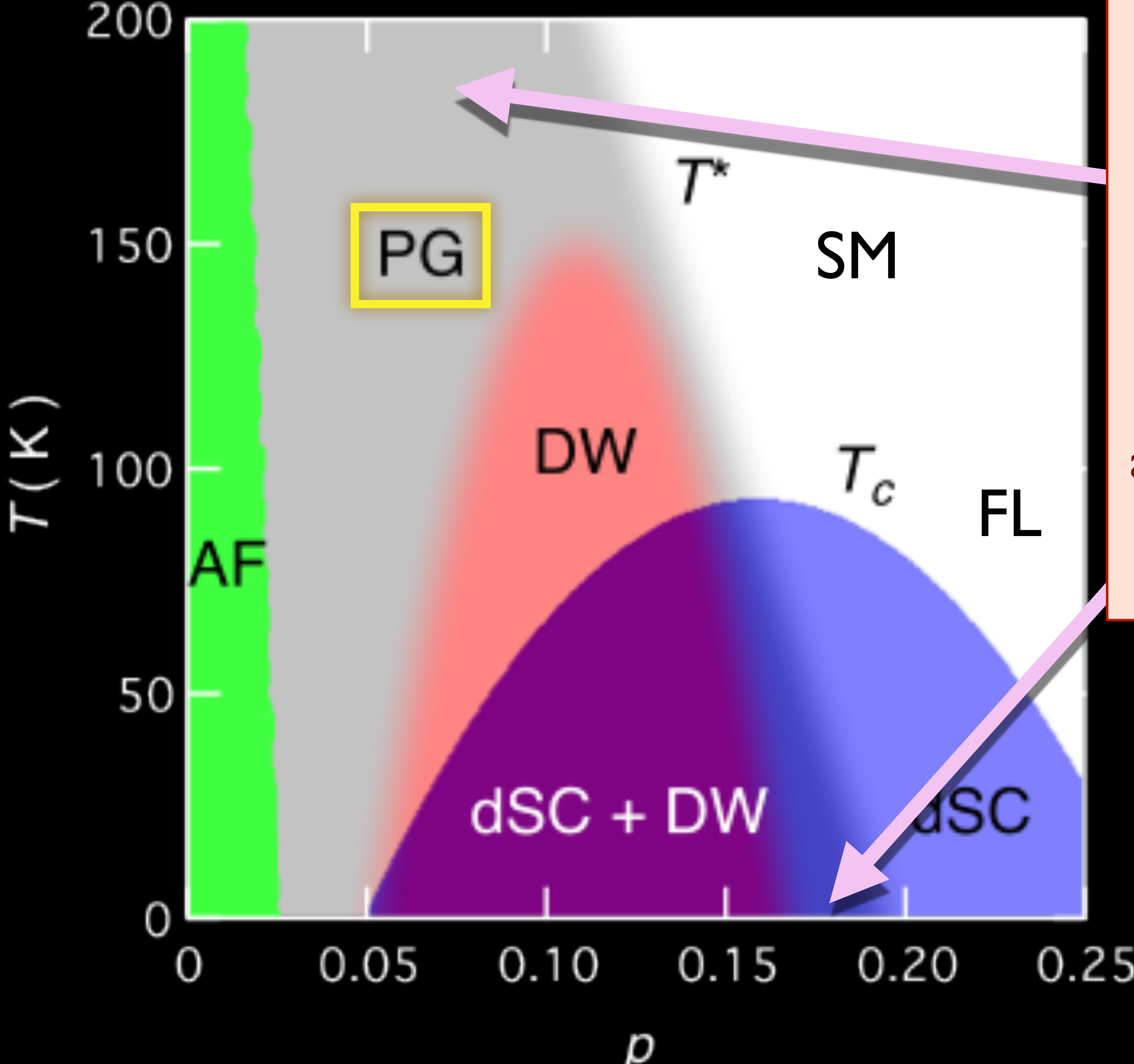

Pseudogap metal at low p

Many indications that this metal behaves like a Fermi liquid, but with Fermi surface size p and *not* $1+p$.

T. Senthil, M. Vojta and S. Sachdev, PRB **69**, 035111 (2004)

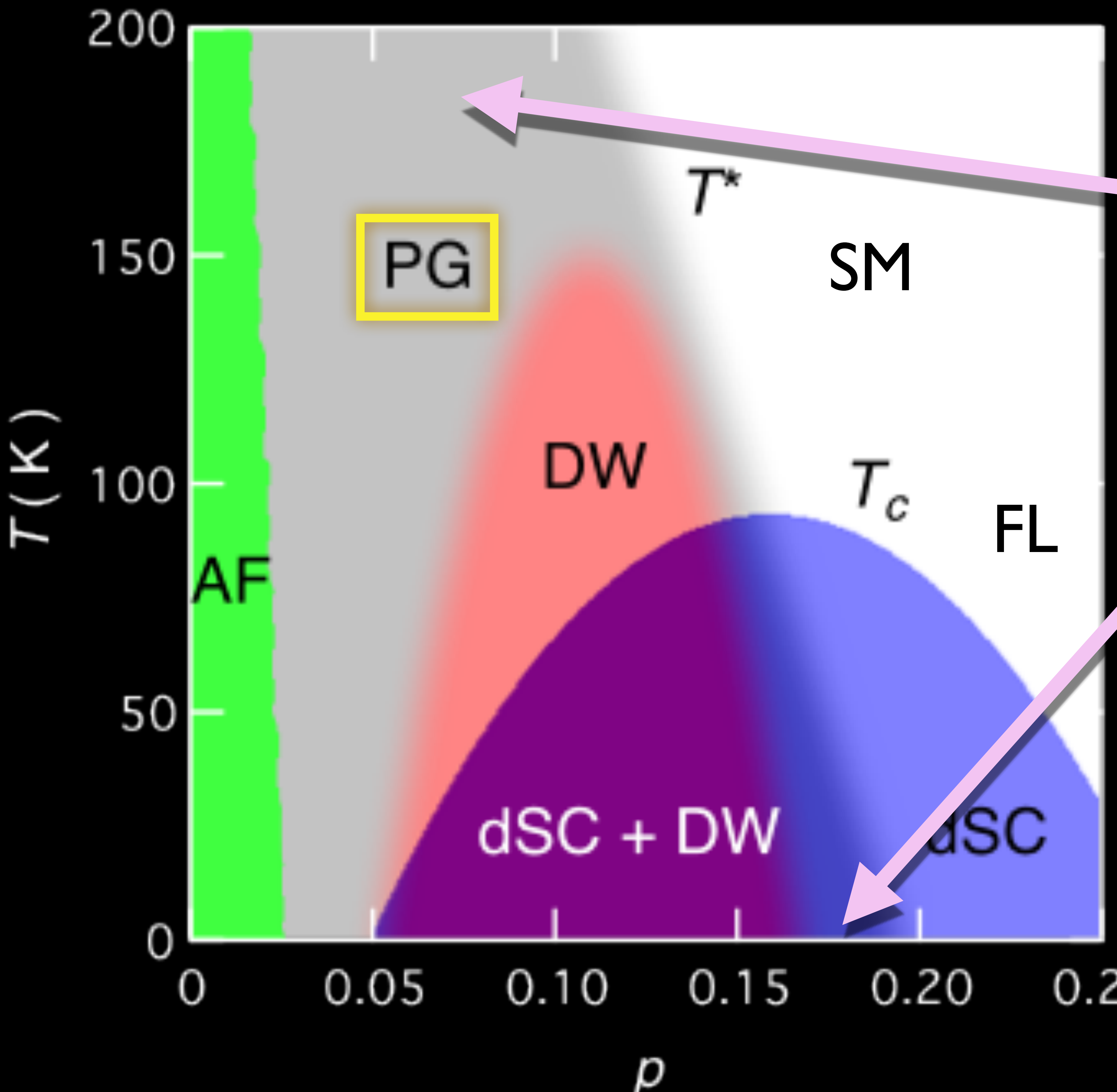

Pseudogap metal at low p

Many indications that this metal behaves like a Fermi liquid, but with Fermi surface size p and *not* $1+p$.

If present at $T=0$, a metal with a size p Fermi surface (and translational symmetry preserved) ***must*** have ***topological order***

Begin with the "spin-fermion" model. **Electrons** $c_{i\alpha}$ on the square lattice with dispersion

$$\mathcal{H}_c = -\sum_{i,\rho} t_\rho \left(c^\dagger_{i,\alpha} c_{i+\boldsymbol{v}_\rho,\alpha} + c^\dagger_{i+\boldsymbol{v}_\rho,\alpha} c_{i,\alpha} \right) - \mu \sum_i c^\dagger_{i,\alpha} c_{i,\alpha} + \mathcal{H}_{\rm int}$$

are coupled to an **antiferromagnetic order parameter** $\Phi^\ell(i)$**,** $\ell = x, y, z$

$$\mathcal{H}_{\rm int} = -\lambda \sum_i \eta_i \Phi^\ell(i) c^\dagger_{i,\alpha} \sigma^\ell_{\alpha\beta} c_{i,\beta} + V_\Phi$$

where $\eta_i = \pm 1$ on the two sublattices.

When $\Phi^\ell(i)$ =constant independent of i, we have long-range AFM, and a gap in the fermion spectrum at the anti-nodes.

Begin with the “spin-fermion” model. **Electrons** $c_{i\alpha}$ on the square lattice with dispersion

$$\mathcal{H}_c = -\sum_{i,\rho} t_\rho \left(c^\dagger_{i,\alpha} c_{i+\boldsymbol{v}_\rho,\alpha} + c^\dagger_{i+\boldsymbol{v}_\rho,\alpha} c_{i,\alpha} \right) - \mu \sum_i c^\dagger_{i,\alpha} c_{i,\alpha} + \mathcal{H}_{\rm int}$$

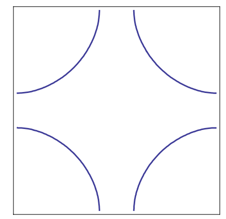

are coupled to an **antiferromagnetic order parameter** $\Phi^\ell(i)$**,** $\ell = x, y, z$

$$\mathcal{H}_{\rm int} = -\lambda \sum_i \eta_i \Phi^\ell(i) c^\dagger_{i,\alpha} \sigma^\ell_{\alpha\beta} c_{i,\beta} + V_\Phi$$

where $\eta_i = \pm 1$ on the two sublattices.

When $\Phi^\ell(i)$ =constant independent of i, we have long-range AFM, and a gap in the fermion spectrum at the anti-nodes.

Begin with the "spin-fermion" model. **Electrons** $c_{i\alpha}$ on the square lattice with dispersion

$$\mathcal{H}_c = -\sum_{i,\rho} t_\rho \left(c^\dagger_{i,\alpha} c_{i+\boldsymbol{v}_\rho,\alpha} + c^\dagger_{i+\boldsymbol{v}_\rho,\alpha} c_{i,\alpha} \right) - \mu \sum_i c^\dagger_{i,\alpha} c_{i,\alpha} + \mathcal{H}_{\rm int}$$

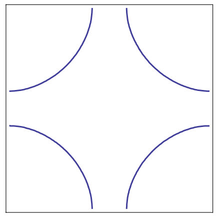

are coupled to an **antiferromagnetic order parameter** $\Phi^\ell(i)$**,** $\ell = x, y, z$

$$\mathcal{H}_{\rm int} = -\lambda \sum_i \eta_i \Phi^\ell(i) c^\dagger_{i,\alpha} \sigma^\ell_{\alpha\beta} c_{i,\beta} + V_\Phi$$

where $\eta_i = \pm 1$ on the two sublattices.

When $\Phi^\ell(i) =$constant independent of i, we have long-range AFM, and a gap in the fermion spectrum at the anti-nodes.

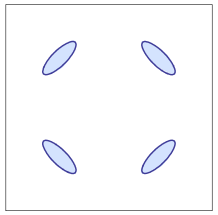

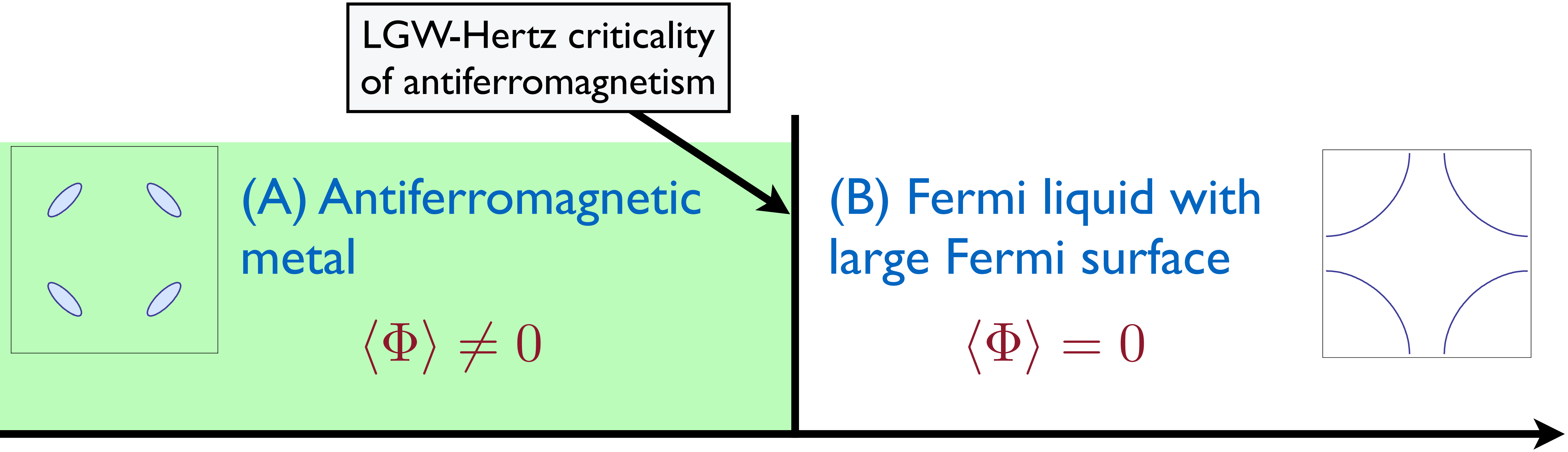
LGW-Hertz criticality
of antiferromagnetism
(A) Antiferromagnetic
metal
$\langle \Phi \rangle \neq 0$
(B) Fermi liquid with
large Fermi surface
$\langle \Phi \rangle = 0$

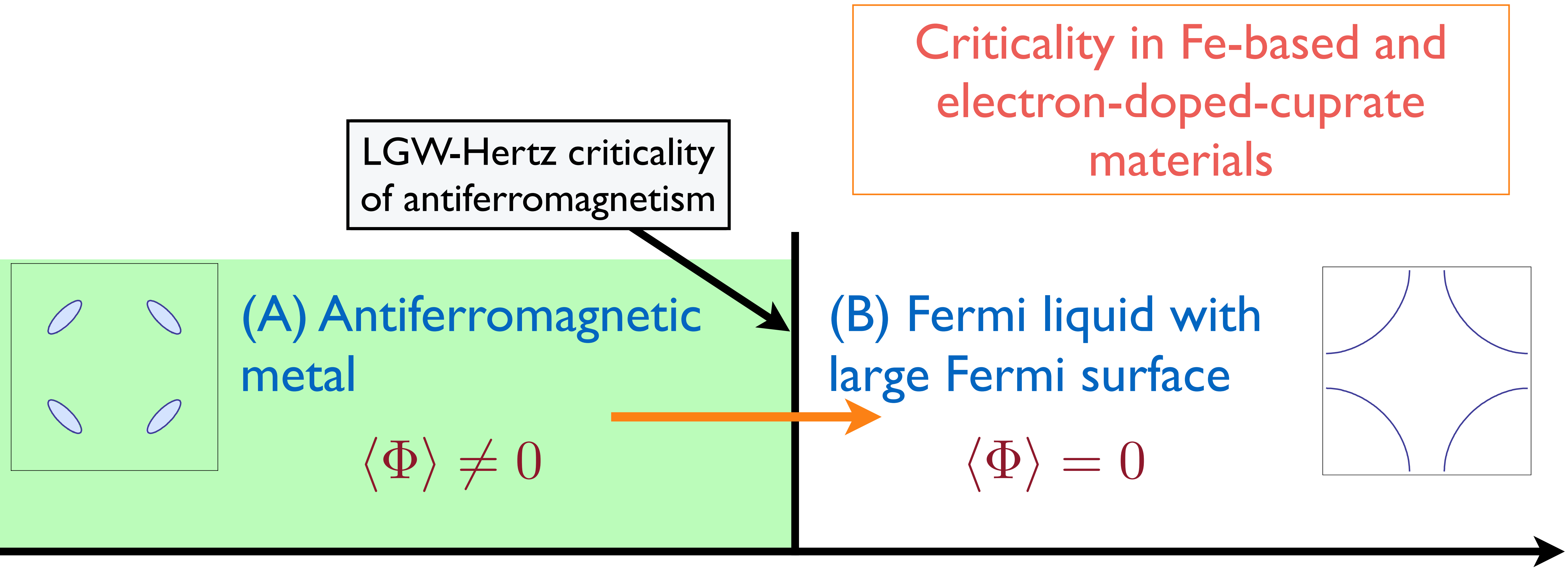
Criticality in Fe-based and electron-doped-cuprate materials
LGW-Hertz criticality of antiferromagnetism
(A) Antiferromagnetic metal
$\langle \Phi \rangle \neq 0$
(B) Fermi liquid with large Fermi surface
$\langle \Phi \rangle = 0$

Can we get a stable zero temperature state with “fluctuating antiferromagnetism” and a small Fermi surface (and so a gap near the anti-nodes) ?

Can we get a stable zero temperature state with "fluctuating antiferromagnetism" and a small Fermi surface (and so a gap near the anti-nodes) ?

Yes, provided the metal has topological order (e.g. Z_2 topological order)

T. Senthil, M. Vojta and S. Sachdev, PRB **69**, 035111 (2004)

For fluctuating antiferromagnetism, we transform to a rotating reference frame using the SU(2) rotation R_i

$$\left(\begin{array}{c} c_{i\uparrow} \\ c_{i\downarrow} \end{array} \right) = R_i \left(\begin{array}{c} \psi_{i,+} \\ \psi_{i,-} \end{array} \right),$$

in terms of fermionic "chargons" ψ_s and a **Higgs field** $H^a(i)$

$$\sigma^\ell \Phi^\ell(i) = R_i \, \sigma^a H^a(i) \, R_i^\dagger$$

The Higgs field is the AFM order in the rotating reference frame.

For fluctuating antiferromagnetism, we transform to a rotating reference frame using the SU(2) rotation R_i

$$\begin{pmatrix} c_{i\uparrow} \\ c_{i\downarrow} \end{pmatrix} = R_i \begin{pmatrix} \psi_{i,+} \\ \psi_{i,-} \end{pmatrix},$$

in terms of fermionic "chargons" ψ_s and a **Higgs field** $H^a(i)$

$$\sigma^\ell \Phi^\ell(i) = R_i \, \sigma^a H^a(i) \, R_i^\dagger$$

The Higgs field is the AFM order in the rotating reference frame. Note that this representation is ambiguous up to a SU(2) gauge transformation, V_i

$$\begin{pmatrix} \psi_{i,+} \\ \psi_{i,-} \end{pmatrix} \rightarrow V_i \begin{pmatrix} \psi_{i,+} \\ \psi_{i,-} \end{pmatrix}$$

$$R_i \rightarrow R_i V_i^\dagger$$

$$\sigma^a H^a(i) \rightarrow V_i \, \sigma^b H^b(i) \, V_i^\dagger.$$

Fluctuating antiferromagnetism

After transforming to the rotating reference frame, the "Yukawa" coupling between the electrons and the spin density wave order becomes the Yukawa coupling between the chargons and the Higgs field

$$\Phi^\ell(i) c^\dagger_{i,\alpha} \sigma^\ell_{\alpha\beta} c_{i,\beta} = H^a(i) \psi^\dagger_{i,s} \sigma^a_{ss'} \psi_{i,s'}$$

Fluctuating antiferromagnetism

The simplest effective Hamiltonian for the fermionic chargons is the same as that for the electrons, with the AFM order replaced by the Higgs field.

$$\mathcal{H}_\psi = -\sum_{i,\rho} t_\rho \left(\psi_{i,s}^\dagger \psi_{i+\boldsymbol{v}_\rho,s} + \psi_{i+\boldsymbol{v}_\rho,s}^\dagger \psi_{i,s} \right) - \mu \sum_i \psi_{i,s}^\dagger \psi_{i,s} + \mathcal{H}_{\rm int}$$

$$\mathcal{H}_{\rm int} = -\lambda \sum_i \eta_i H^a(i) \psi_{i,s}^\dagger \sigma^a_{ss'} \psi_{i,s'} + V_H$$

Fluctuating antiferromagnetism

The simplest effective Hamiltonian for the fermionic chargons is the same as that for the electrons, with the AFM order replaced by the Higgs field.

$$\mathcal{H}_\psi = -\sum_{i,\rho} t_\rho \left(\psi^\dagger_{i,s} \psi_{i+\boldsymbol{v}_\rho, s} + \psi^\dagger_{i+\boldsymbol{v}_\rho, s} \psi_{i,s} \right) - \mu \sum_i \psi^\dagger_{i,s} \psi_{i,s} + \mathcal{H}_{\rm int}$$

$$\mathcal{H}_{\rm int} = -\lambda \sum_i \eta_i H^a(i) \psi^\dagger_{i,s} \sigma^a_{ss'} \psi_{i,s'} + V_H$$

IF we can transform to a rotating reference frame in which $H^a(i) =$ a constant independent of i and time, **THEN** the ψ fermions in the presence of fluctuating AFM will inherit the anti-nodal gap of the electrons in the presence of static AFM.

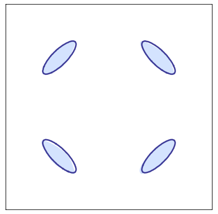

Lattice gauge theory

Field	Symbol	Statistics	$SU(2)_{\text{gauge}}$	$SU(2)_{\text{spin}}$	$U(1)_{\text{e.m.charge}}$
Electron	c	fermion	$\mathbf{1}$	$\mathbf{2}$	-1
Spin magnetic moment	Φ	boson	$\mathbf{1}$	$\mathbf{3}$	0
Chargon	ψ	fermion	$\mathbf{2}$	$\mathbf{1}$	-1
Spinon	R or z	boson	$\bar{\mathbf{2}}$	$\mathbf{2}$	0
Higgs	H	boson	$\mathbf{3}$	$\mathbf{1}$	0

Lattice gauge theory

Field	Symbol	Statistics	$SU(2)_{\text{gauge}}$	$SU(2)_{\text{spin}}$	$U(1)_{\text{e.m.charge}}$
Electron	c	fermion	$\mathbf{1}$	$\mathbf{2}$	-1
Spin magnetic moment	Φ	boson	$\mathbf{1}$	$\mathbf{3}$	0
Chargon	ψ	fermion	$\mathbf{2}$	$\mathbf{1}$	-1
Spinon	R or z	boson	$\bar{\mathbf{2}}$	$\mathbf{2}$	0
Higgs	H	boson	$\mathbf{3}$	$\mathbf{1}$	0

- Higgs phase: $\langle H \rangle \neq 0$ leads to reconstructed "small" Fermi surfaces. Because $H \in SO(3)$ and $\pi_1(SO(3)) = Z_2$ there can be Z_2 flux through the hole of a torus *i.e.* Z_2 topological order.

- Confining phase: Color superconductor —model of the overdoped superconductor.

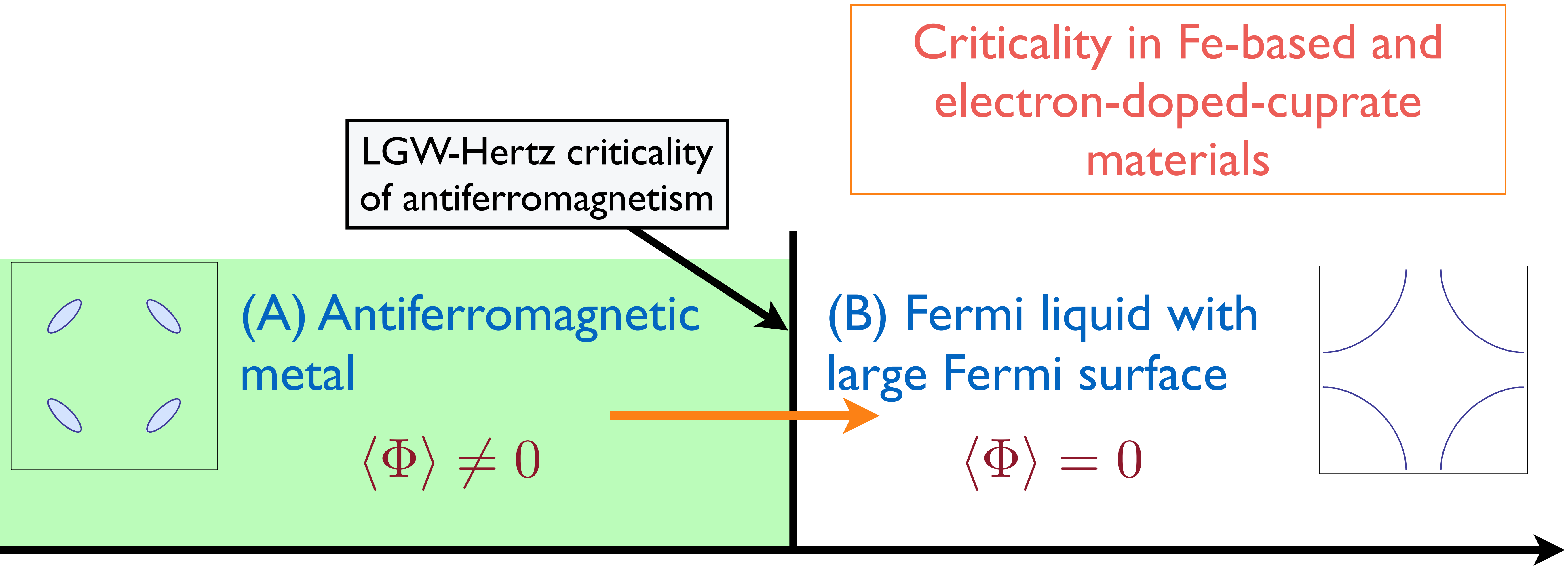
Criticality in Fe-based and electron-doped-cuprate materials
LGW-Hertz criticality of antiferromagnetism
(A) Antiferromagnetic metal
$\langle \Phi \rangle \neq 0$
(B) Fermi liquid with large Fermi surface
$\langle \Phi \rangle = 0$

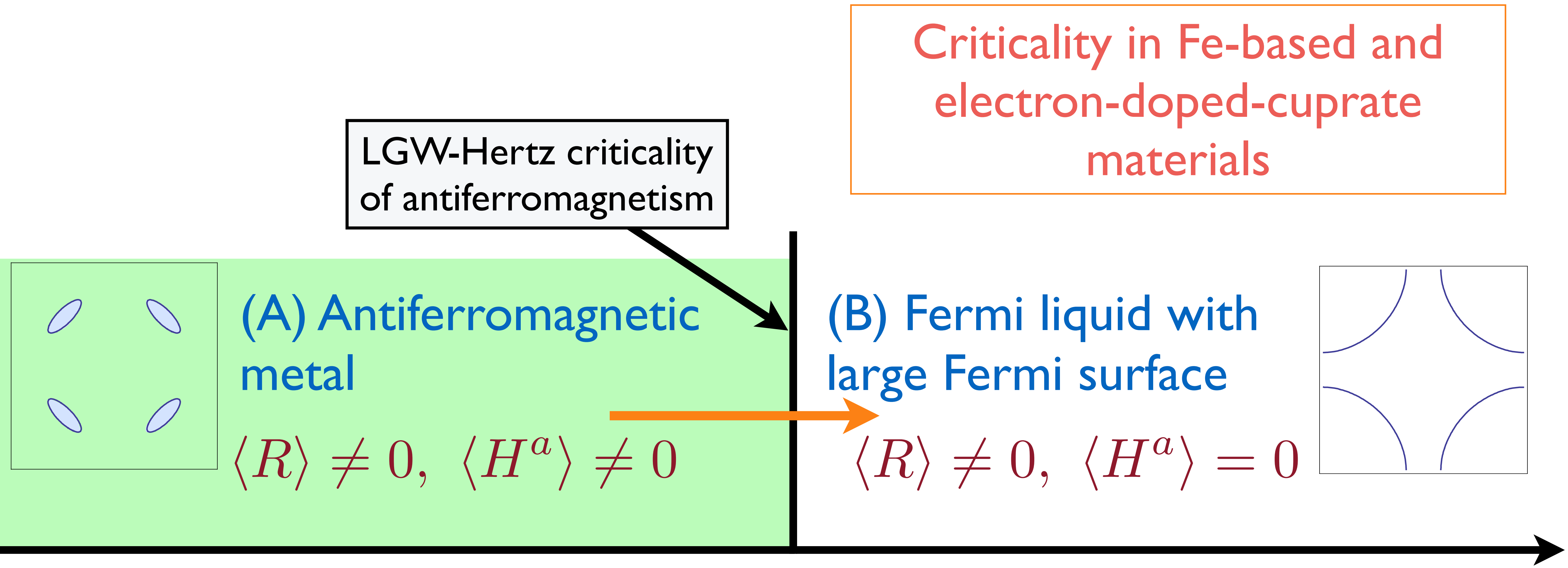
Criticality in Fe-based and electron-doped-cuprate materials
LGW-Hertz criticality of antiferromagnetism
(A) Antiferromagnetic metal
$\langle R \rangle \neq 0, \ \langle H^a \rangle \neq 0$
(B) Fermi liquid with large Fermi surface
$\langle R \rangle \neq 0, \ \langle H^a \rangle = 0$

Global phase diagram

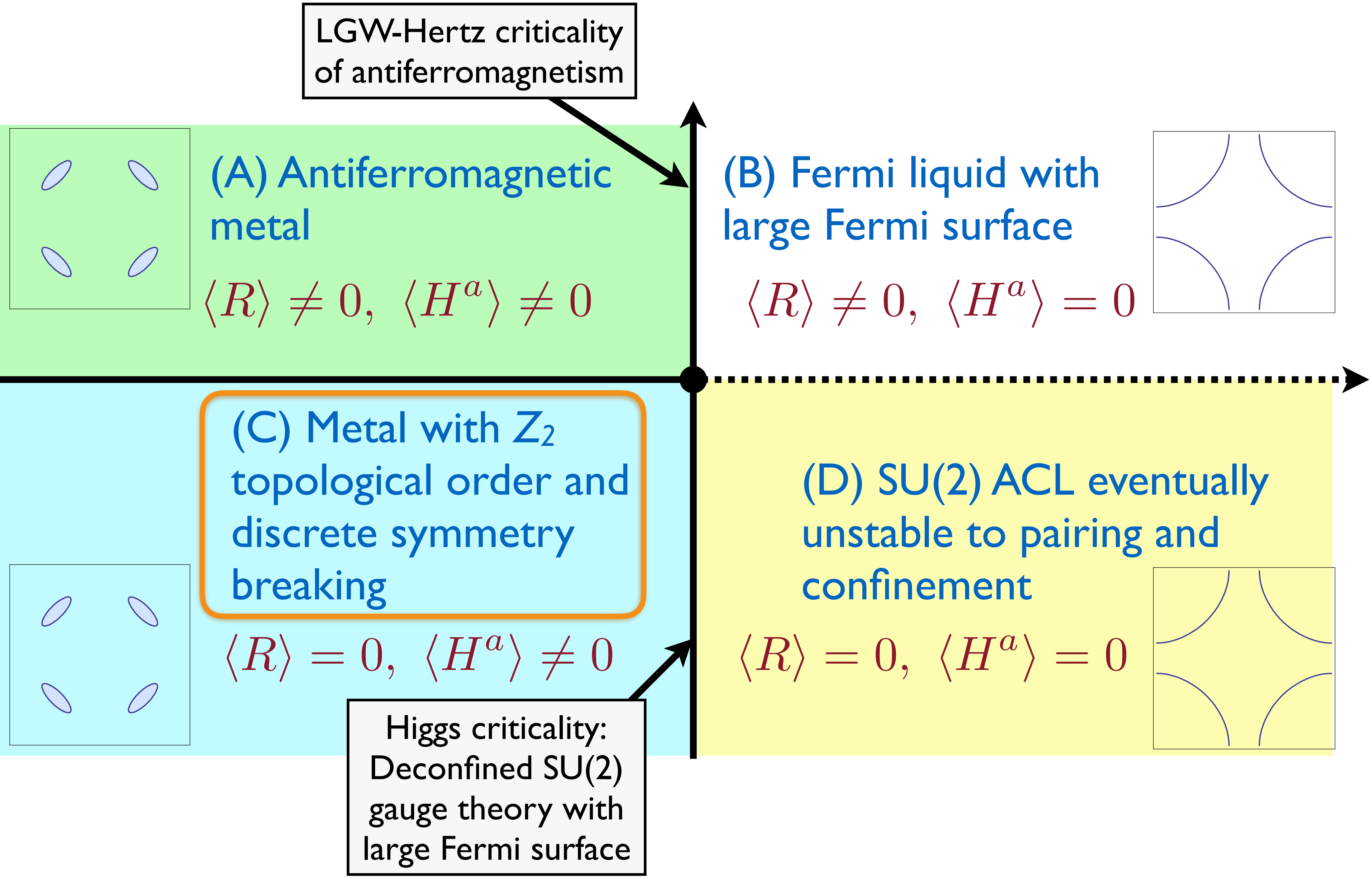

Global phase diagram

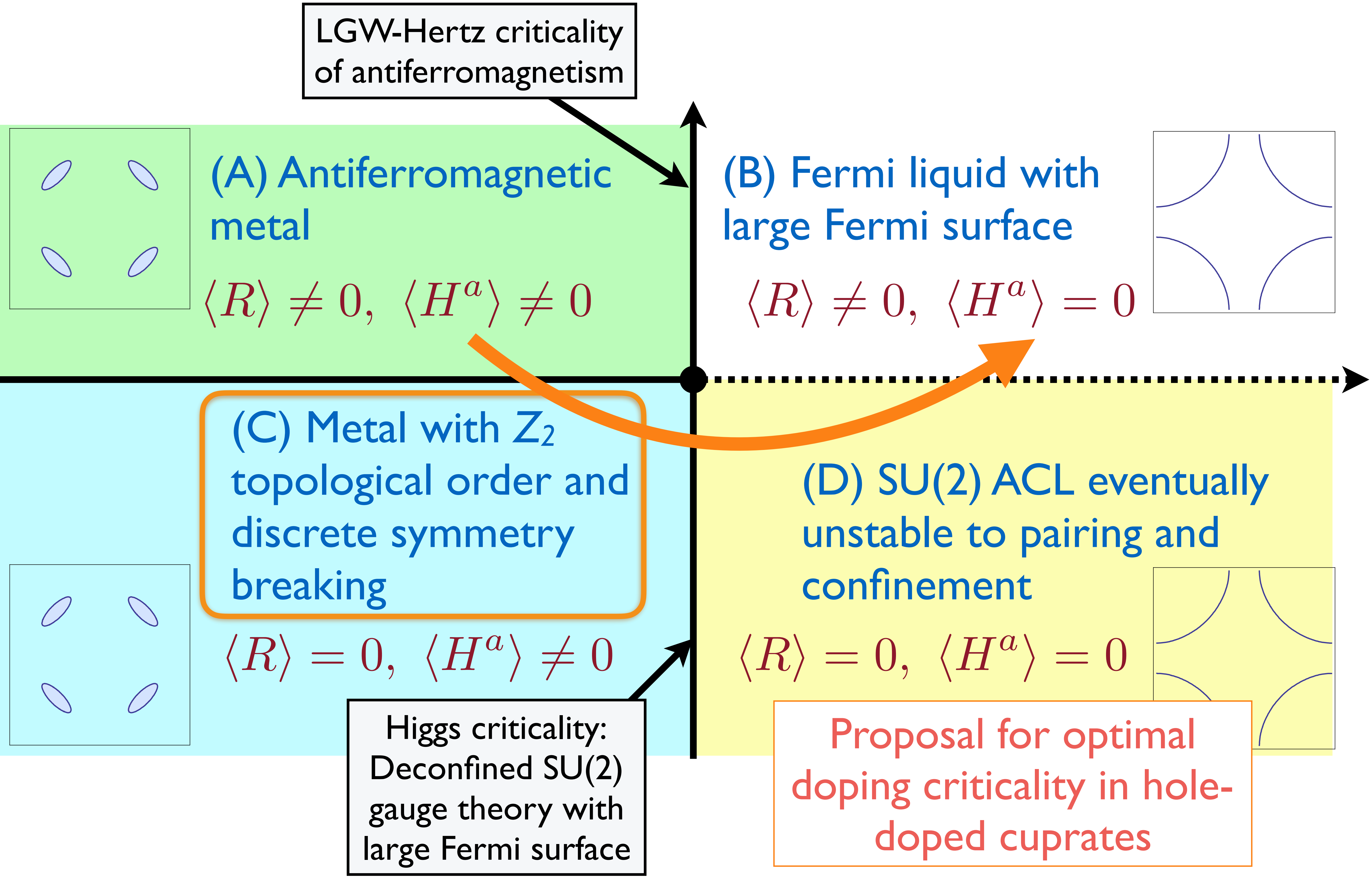

S. Sachdev and S. Chatterjee, arXiv:1703.00014

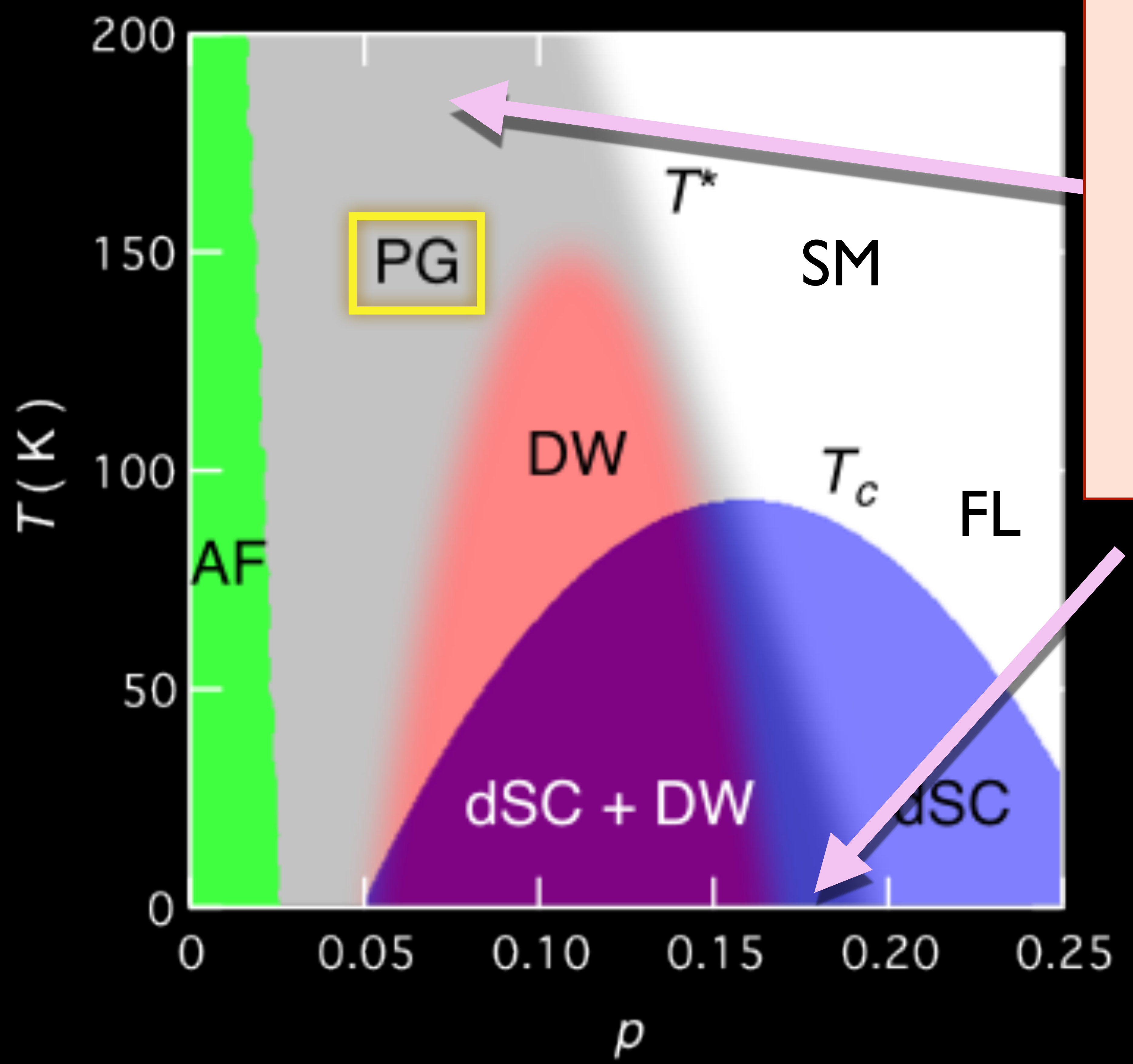

Pseudogap metal at low p

Lattice gauge theory for a metal with topological order

S. Sachdev, M. A. Metlitski, Y. Qi, and C. Xu, PRB **80**, 155129 (2009); D. Chowdhury and S. Sachdev, PRB **91**, 115123 (2015); S. Sachdev and D. Chowdhury, arXiv:1605.03579.

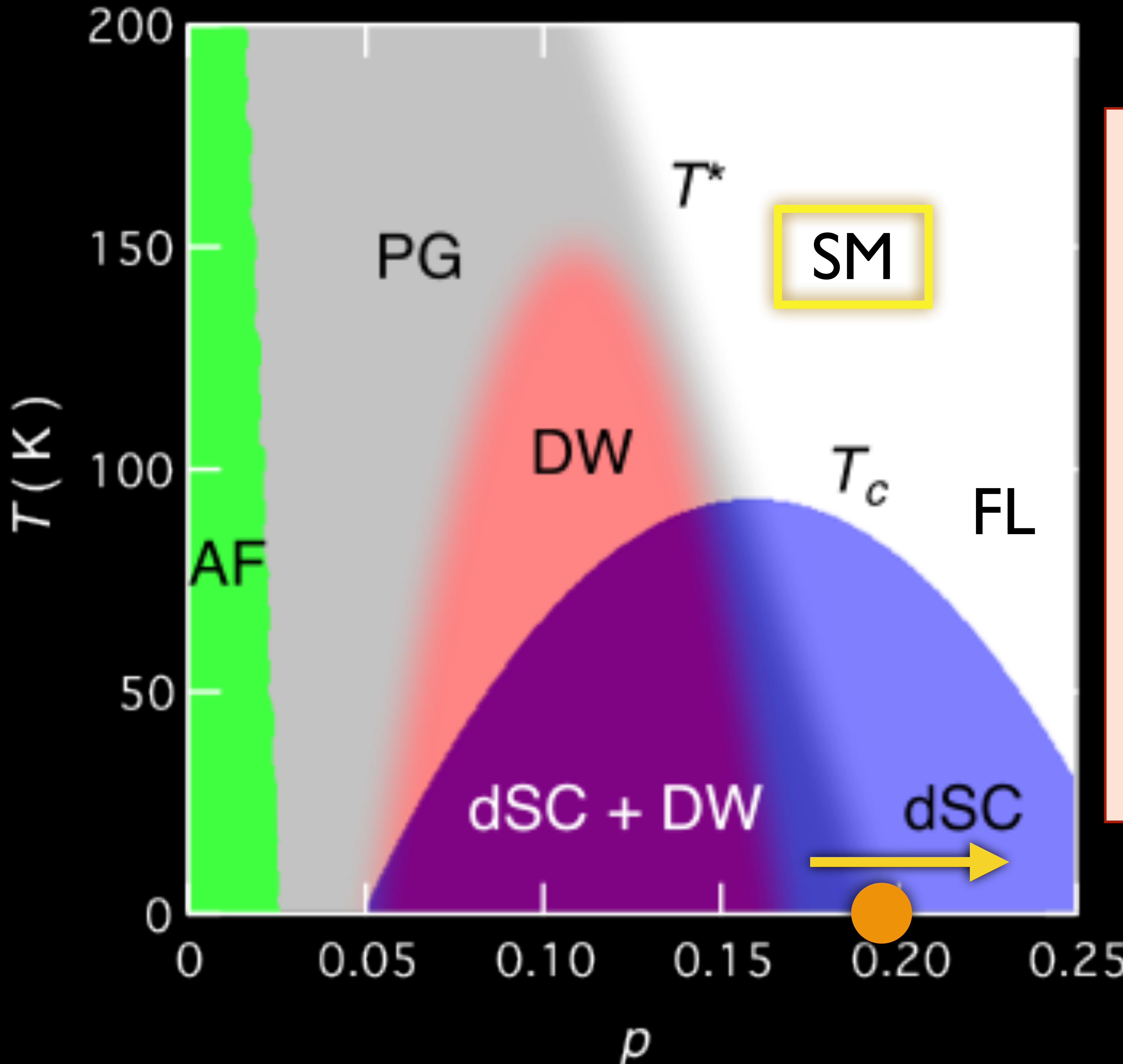

Gauge theory for a topological phase transition, and for the strange metal (SM)